

Runaway breakdown and electric discharges in thunderstorms

A V Gurevich, K P Zybin

DOI: 10.1070/PU2001v044n11ABEH000939

Contents

1. Introduction	1119
2. Runaway breakdown (elementary theory)	1120
3. Kinetic equation for fast electrons in matter	1122
3.1 Kinetic equation; 3.2 Collision integral; 3.3 Ionization integral; 3.4 Spherically symmetric distribution function; 3.5 The general form of the ionization integral	
4. Runaway breakdown (kinetic theory)	1125
4.1 Statement of the problem; 4.2 The structure of the distribution function; 4.3 The time of exponential growth; 4.4 Analysis of the asymptotic behavior of the distribution function; 4.5 Spatially nonuniform breakdown; 4.6 Runaway avalanches in a nonuniform electric field	
5. Conditions for the occurrence of runaway breakdown in the atmosphere	1130
6. High-altitude atmospheric discharges	1131
6.1 Optical observations of high-altitude discharges; 6.2 Radio observations at very low frequencies; 6.3 A model of high-altitude discharge; 6.4 A model of optical emission; 6.5 Gamma-ray bursts; 6.6 High-energy electrons in the magnetosphere; 6.7 Generation of electron–positron pairs	
7. Lightning discharges in the atmosphere	1134
7.1 Maximum electric field; 7.2 Anomalous X-ray bursts; 7.3 Anomalous growth of conductivity; 7.4 Radio-interferometric measurements; 7.5 Generation of a lightning	
8. Cosmic rays and electrodynamic processes in the Earth's atmosphere	1137
9. Laboratory experiment	1138
10. Conclusion	1138
References	1139

Abstract. This review concerns the theory of the avalanche multiplication of high-energy (0.1–10 MeV) electrons in a neutral material, a newly discovered phenomenon known as runaway breakdown (RB). In atmospheric conditions RB takes place at electric fields an order of magnitude weaker than those needed for normal breakdown in air. Experimental work of the past few years has shown that RB determines the maximum electric field strength in thunderclouds and is behind a variety of phenomena newly observed in thunderstorm atmosphere, such as giant high-altitude discharges between thunderclouds and the ionosphere, anomalous amplifications of X-ray emission, intense bursts of gamma radiation, etc. These phenomena are becoming increasingly active areas of study. A necessary condition for the occurrence of runaway avalanche is the presence of high energy seed electrons. In the atmosphere, these are cosmic ray secondary electrons. Therefore, the observed effects reflect the close relationship between cosmic rays and electrodynamic processes in the thunderstorm atmosphere.

The first laboratory results on RB are also presented. Further studies in this area may be of interest for high-current electronics.

1. Introduction

The generation of an electric discharge in matter, i.e., an electric breakdown has been studied for over two centuries. It has been investigated in detail and has various technical applications [2–8]. However, the process which the present review is devoted to was discovered in recent years. This new physical phenomenon has been called *runaway breakdown* [1].

The conventional breakdown results from the heating of electrons in an electric field. In this process, fast electrons that belong to the tail of the distribution function become able to ionize matter and, therefore, to generate new free electrons. Slow electrons disappear owing to recombination in the bulk or on the walls of the discharge chamber. As soon as the electric field becomes sufficiently strong, the generation of new electrons due to ionization exceeds their disappearance due to recombination, and their number begins exponentially increasing. This phenomenon is termed the electrical breakdown of matter. The characteristic energies of the electrons responsible for ionization are 10–20 eV, while recombination mostly takes place at low energies. For this reason, the mean electron energy $\bar{\epsilon}$ at which breakdown occurs does not normally exceed several electron-volts. For instance, in air this energy is $\bar{\epsilon} \sim 2$ eV.

A V Gurevich, K P Zybin P N Lebedev Physics Institute,
Russian Academy of Sciences
Leninskii prosp. 53, 117924 Moscow, Russian Federation
Tel. (7-095) 132 61 71
E-mail: alex@lpi.ru; zybin@lpi.ru

Received 26 January 2001, revised 26 June 2001
Uspekhi Fizicheskikh Nauk 171 (11) 1177–1199 (2001)
Translated by M V Tsaplina; edited by A V Getling

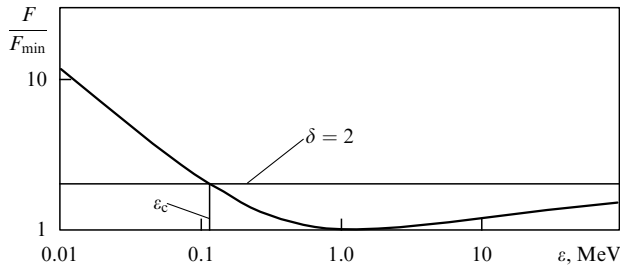


Figure 1. Dependence of the braking force F on the electron energy ε . The force F is normalized to F_{\min} , and the parameter δ is equal to E/E_c .

The runaway breakdown has an essentially different nature, which is based on the specific features of the fast particle–matter interaction. The braking force F acting on an energetic particle in matter is determined by the ionization losses [9]. Figure 1 shows that the force F decreases with increasing electron energy ε . The reason is that a fast electron interacts with electrons and nuclei of neutral matter as if they were free particles, i.e., according to the Coulomb law. The Coulomb scattering cross section is the Rutherford cross section $\sigma \sim 1/\varepsilon^2$. That is why, in the nonrelativistic region, the braking force is $F \sim \varepsilon \sigma N_m \sim 1/\varepsilon$, i.e., is proportional to the molecular density N_m and inversely proportional to the electron energy. The decrease in the ionization braking force becomes weaker owing to relativistic effects. For $\varepsilon \geq 1$ MeV it reaches its minimum F_{\min} , and then a logarithmically slow increase begins (see Fig. 1).

The decrease in the friction force is related to the possibility of the appearance of runaway electrons in a substance placed in an electric field. Indeed, if a constant field E is present in a medium, such that $E > E_c = F_{\min}/e$, an electron with a sufficiently high energy $\varepsilon > \varepsilon_c$, where the critical runaway energy is

$$\varepsilon_c \approx \frac{E_c}{2E} mc^2,$$

will be continuously accelerated by the field (see Fig. 1). Such electrons are called runaway electrons. Many studies [10–12], both theoretical and experimental, have been devoted to them (e.g., in toroidal units for controlled thermonuclear fusion).

The runaway breakdown is related to the generation of secondary electrons due to the fast-runaway-particle ionization of neutral molecules. Although the bulk of secondary electrons have low energies, electrons with a rather high energy $\varepsilon > \varepsilon_c$ can also be produced. These will also become runaway electrons, i.e., they will be accelerated by the field (see Fig. 1) and, in the ionization process, may in turn generate particles with $\varepsilon > \varepsilon_c$. As a result, an exponentially growing runaway avalanche appears. In parallel, a large number of slow electrons are generated, which ultimately leads to an electrical breakdown of the matter. It is of importance that runaway breakdown occurs in a relatively weak field $E \geq E_c$, which is an order of magnitude smaller than the threshold field E_{th} for conventional breakdown. For instance, in air at the atmospheric pressure, we have $E_{th} \simeq 23 \text{ kV cm}^{-1}$ and $E_c \simeq 2.16 \text{ kV cm}^{-1}$.

However, the condition $E > E_c$ alone is insufficient for a runaway breakdown. The presence of fast seed electrons with energies exceeding the critical runaway energy $\varepsilon > \varepsilon_c \geq (0.1–1 \text{ MeV})$ is necessary. What is even more important is that the spatial scale L of the constant electric

field in the matter must substantially exceed the characteristic length of the exponential growth of the runaway avalanche, l_a : $L \gg l_a$. The latter quantity proves to be very large in gas media, which is the main obstruction to the realization of the effect in question under laboratory conditions. For example, in air under the atmospheric pressure, we have $l_a \sim 50 \text{ m}$.

At the same time, the situation is radically different in the thunderstorm atmosphere. The characteristic sizes of clouds L are there always much greater than l_a . Fast seed electrons are also constantly present, for they are effectively generated by cosmic rays [the flux density of secondary electrons of cosmic rays with energies $E \geq 1 \text{ MeV}$ is of the order of $10^3 \text{ particles (m}^2 \text{ s)}^{-1}$]. Therefore, runaway breakdown is quite possible in thunderclouds as soon as the electric field reaches the value E_c . As measurements show, such fields are actually present. It is runaway breakdown that plays a significant role in the recently discovered remarkable phenomena such as giant high-altitude discharges (‘sprites’) between thunderclouds and the ionosphere, powerful gamma-ray and X-ray bursts, and others.

Attention should also be given to the specific physics underlying these processes. The atmosphere is a rather dense medium, where the free paths of both neutral molecules and thermal electrons are only thousandths of a millimeter and the lifetime of free electrons is tens of nanoseconds. In spite of this, giant *macroscopic* (kilometer- and even several-kilometer-scaled) processes determined by purely *kinetic* effects occur in relatively weak electric fields. This is a really wonderful physical phenomenon.

In this review we elucidate the current state of the theory of runaway breakdown and its manifestations in the thunderstorm atmosphere. In Section 2 we briefly present a simple physical theory of runaway breakdown. A consistent kinetic theory is given at length in Section 3. There we formulate the kinetic equation and derive expressions for all collision integrals, including the ionization integral and the integrals of generation of radiation and electron–positron pairs. Section 4 presents numerical and analytical solutions to the kinetic equation. Different asymptotics are obtained for the distribution function. The parameter of the exponential growth and the characteristic spatial scale of the avalanche of fast electrons are determined. Conditions for the occurrence of a runaway breakdown in the thunderstorm atmosphere are analyzed in Section 5. In Section 6 we briefly describe observational data on giant high-altitude discharges (sprites) and compare them with the results of theoretical simulations. In Section 7 the results of the theory are compared with new observational data on lightning discharges in thunderclouds obtained using airplanes and probe balloons. The fundamentally important role of cosmic rays in the generation of a runaway breakdown is stressed in Section 8, which describes the results of experiments carried out on special high-altitude stands during thunderstorms. Section 9 gives the results of runaway-breakdown simulations in laboratory conditions using the cyclotron resonance phenomenon. In conclusion, possibilities of the realization of the effect under study in dense media are briefly discussed. The implementation of such a project would have interesting prospects for various applications.

2. Runaway breakdown (elementary theory)

Runaway breakdown was first predicted theoretically by A V Gurevich, G M Milikh, and R A Roussel-Dupre in

1992 [1]. This phenomenon has its origins in the interaction of fast particles with matter. The braking force F acting on an energetic particle in matter is determined by the ionization losses described by the well-known Bethe formulas [9] and has the form given in Fig. 1. In the nonrelativistic region, which is of greatest interest for us, F is specified by the simple formula [13]:

$$F = \frac{2\pi e^4 Z N_m}{\varepsilon} \ln \frac{\varepsilon}{J_z}. \quad (1)$$

Here ε is the particle energy, N_m is the molecule density, Z is the average number of electrons in a molecule, and J_z is an energy of the order of $Z\varepsilon_i$ (ε_i is the ionization energy). The equation shows that the force F decreases with increasing electron energy. This is due to the specific features of the Coulomb interaction (see Fig. 1). The decrease in the braking force becomes smaller owing to relativistic effects, and for $\varepsilon = 1.4$ MeV the force reaches its minimum value

$$F_{\min} = \frac{4\pi e^4 Z N_m}{mc^2} a, \quad a \approx 11. \quad (2)$$

Further, it increases slowly (logarithmically) with increasing ε .

Runaway electrons can be generated in the region where the friction force decreases. If a constant field of strength

$$E > E_c = \frac{F_{\min}}{e} = \frac{4\pi e^3 Z N_m}{mc^2} a \quad (3)$$

is present in a medium, an electron with a sufficiently high energy $\varepsilon > \varepsilon_c$, where

$$\varepsilon_c \approx \frac{E_c}{2E} mc^2, \quad (4)$$

will be continuously accelerated by this field (see Fig. 1). The possibility of runaway for fast electrons in the atmosphere under the influence of thunderstorm fields was first pointed out by Wilson [14].

As shown in the introduction, the generation of secondary electrons via ionization of neutral molecules by fast particles can induce an exponentially growing avalanche of runaway electrons.

Note that, in a very strong field corresponding to the *maximum* braking force $F_{\max} \approx eE_{\text{cn}}$ in a neutral gas [10],

$$E \geq E_{\text{cn}} = \frac{4\pi e^3 Z N_m}{2.72 \tilde{\varepsilon}}; \quad \tilde{\varepsilon} \approx J_z = Z\varepsilon_i,$$

all plasma electrons quickly pass over to the acceleration regime. High fields close to E_{cn} are used in high-current electronics [2, 15]. The critical field for the runaway breakdown considered here corresponds to the *minimum* braking force (2). The critical-field-strength ratio is

$$\frac{E_{\text{cn}}}{E_c} = \frac{F_{\max}}{F_{\min}} \approx \frac{mc^2}{2.72a \tilde{\varepsilon}} \approx 200.$$

Thus, runaway breakdown occurs in a relatively weak field, which is much weaker than not only E_{cn} but also the threshold field E_{th} of normal breakdown.

The runaway breakdown theory has been developed both in an elementary hydrodynamic approximation [1, 16] and in the framework of a consistent kinetic theory [17–24].

We shall first consider a simple elementary theory. In this case, a leading role is played by electrons of energy ε close to ε_c (4). Indeed, the motion of an electron in the direction of a constant electric field E is described by the equation

$$m \frac{dv}{dt} = eE\mu - F(\varepsilon), \quad (5)$$

where $F(\varepsilon)$ is the braking force (1) acting on the electron and μ is the cosine of the angle between the direction of the electron velocity \mathbf{v} and the direction of the electric field \mathbf{E} . Considering for simplicity the motion along the field ($\mu = 1$), we obtain from (5)

$$\frac{d\varepsilon}{dt} = e\sqrt{\frac{2\varepsilon}{m}} \left(E - \frac{F(\varepsilon)}{e} \right). \quad (6)$$

It follows from (6) and (1)–(4) that the field strength is $E > F(\varepsilon)/e$ for electrons with energies $\varepsilon > \varepsilon_c$, and these electrons accelerate, i.e., become runaway electrons. On the contrary, $E < F/e$ for $\varepsilon < \varepsilon_c$, and such electrons decelerate rapidly.

We now take into account that fast electrons in matter lose their energy basically as a result of the ionization of molecules [9]. The ionization releases a new electron of energy ε_1 . The number of electrons with energies exceeding ε_1 that are produced through the ionization of molecules by a fast particle of energy $\varepsilon \gg \varepsilon_1$ per unit length ds is determined by the formula [13]

$$\frac{dN(\varepsilon_1)}{ds} = \frac{\pi Z N_m e^4}{mc^2 \varepsilon_1}. \quad (7)$$

If $\varepsilon_1 \geq \varepsilon_c$, all newly produced electrons become runaway electrons. Then the characteristic length of runaway-electron generation can be determined from (4) and (7):

$$l_a = \left(\frac{dN}{ds} \right)_{\varepsilon_1 = \varepsilon_c}^{-1} = \frac{(mc^2)^2}{2\pi Z N_m e^4} \frac{E_c}{E}.$$

The total growth of the number of runaway electrons will then be described by the expression

$$\frac{dN}{ds} = \frac{1}{l_a} N_f, \quad (8)$$

where N_f is the number of fast electrons with energies $\varepsilon > \varepsilon_c$. We now take into account the fact that fast electrons N_f are the same as runaway electrons, but additionally accelerated by the electric field. Let us introduce the characteristic acceleration length s_0 over which an electron gains an energy ε_c . Then, if a newly produced electron has the energy ε_c , at a distance of s_0 it will already have $2\varepsilon_c$ and will therefore be able to produce an electron of energy ε_c , remaining a runaway electron ($\varepsilon \geq \varepsilon_c$). In other words, $N_f = N(s - s_0)$ in equation (21), which can thus be rewritten as

$$\frac{dN}{ds} = \frac{N(s - s_0)}{l_a}.$$

The solution of this equation is

$$N = N_0 \exp \frac{s}{l_1},$$

where the parameter l_1 is specified by the relation

$$\frac{l_1}{l_a} \exp\left(-\frac{s_0}{l_1}\right) = 1.$$

From this, assuming that $s_0/l_1 \ll 1$ (this condition is typically well satisfied [1]), we obtain

$$N = N_0 \exp \frac{s}{l_1}, \quad l_1 = l_a \left(1 + \frac{s_0}{l_1}\right) \simeq l_a.$$

Thus, in the conditions considered, runaway electrons form an avalanche, which grows exponentially over the characteristic length l_a . In particular, for air we have

$$l_a = \frac{(mc^2)^2}{2\pi N_m Z e^4} \frac{E_c}{E} \simeq 50 \text{ m} \times \frac{E_c}{E} \left(\frac{N_m}{2.7 \times 10^{19} \text{ cm}^{-3}} \right)^{-1}. \quad (9)$$

Along with runaway electrons, the number of slow thermal electrons also increases exponentially. Their number is of course much larger than that of runaway electrons. This leads to a rapid growth in the electrical conductivity of the medium, that is, to an electrical breakdown. We emphasize that, as can be seen from (9), in the atmosphere near the Earth's surface, the characteristic length of the avalanche due to a runaway breakdown is several tens of meters. It increases further with height (because of the decrease in N_m).

3. Kinetic equation for fast electrons in matter

3.1 Kinetic equation

The elementary runaway-breakdown theory presented above is extremely simplified. It considers the braking of only one electron and disregards the scattering of fast electrons by electrons and the nuclei of molecules, radiation losses, and the energy and momentum distribution function of fast electrons.

Furthermore, the X-ray and γ -ray quanta emitted by fast electrons can in themselves ionize molecules and, when interacting with molecular nuclei, produce electron–positron pairs. Thus, a whole complex of associated processes induced by relativistic runaway electrons and by the radiation generated by these electrons occur in a constant electric field. Certainly, an exhaustive description of these processes can only be given within the framework of a consistent kinetic theory, with a simultaneous consideration of the kinetic equations for electrons, photons, and positrons.

However, this general system of equations can be substantially simplified for the theory of the phenomenon of interest, namely, runaway breakdown (RB). The point is that RB is determined by ionization processes. At the same time, the emission of photons and, accordingly, photoionization is parametrically weaker than the ionization by head-on electron impact: the small parameter is the fine-structure constant [25]

$$\alpha = \frac{e^2}{\hbar c} = \frac{1}{137}. \quad (10)$$

The same refers to the generation of electron–positron pairs [25]. No less important is the specific behavior of the electron distribution function. As will be shown below, as an RB takes place, the distribution function in the nonrelativistic region increases very rapidly with decreasing electron energy ε . As a

result, the overwhelming contribution to the generation of runaway electrons comes from the region of energies close to the critical runaway energy $\varepsilon \sim \varepsilon_c$ (4). In this energy range, only the ionization by head-on electron impact is important — the so-called ionization loss of fast electrons in matter.

Hence, the leading contribution to the runaway breakdown is made by the ionization loss, which means that the process in question can be described by a single equation for fast electrons in matter:

$$\frac{\partial f}{\partial t} + \mathbf{p} \frac{\partial f}{\partial \mathbf{r}} + e\mathbf{E} \frac{\partial f}{\partial \mathbf{p}} = S(f, F_m). \quad (11)$$

Here $f(\mathbf{r}, \mathbf{p}, t)$ is the distribution function of electrons over coordinates \mathbf{r} and momenta \mathbf{p} , E is the electric field strength, and S is the collision integral dependent on the distribution function of electrons, f , and neutral molecules, F_m .

3.2 Collision integral

The collision integral for fast electrons in matter, $S(f, F_m)$, can be represented as

$$S(f, F_m) = \text{St}(f) + S_I(f) + S_1(f). \quad (12)$$

Here, $\text{St}(f)$ describes the energy loss and the scattering of fast electrons due to collisions with molecules, $S_I(f)$ is the ionization integral describing the production of new electrons, and $S_1(f)$ describes the generation of electron–positron pairs.

It is of importance that, for the considered process of runaway breakdown, the high-energy electron density N_e is much lower than the density N_m of neutral molecules. This means that the Boltzmann collision integral can be represented in the linear form

$$S(f, F_m) = \iint d\mathbf{v}_1 d\Omega u [q_-(u, \theta) f(\mathbf{v}) F_m(\mathbf{v}_1) - q_+(u, \theta) f(\mathbf{v}') F_m(\mathbf{v}_1')]. \quad (13)$$

Here \mathbf{v}' , \mathbf{v} and \mathbf{v}_1' , \mathbf{v}_1 are the velocities of electrons and molecules, respectively, before and after the collision, $u = |\mathbf{v} - \mathbf{v}_1|$, θ is the angle between \mathbf{u} and $\mathbf{v}' - \mathbf{v}_1'$, and $q_{\pm}(\theta, u)$ is the differential cross section of collision.

Moreover, since we consider the kinetic equation only for high-energy electrons with $\varepsilon \gg \varepsilon_i$, where ε_i is the ionization energy, the small parameter

$$\frac{\varepsilon_i}{\varepsilon} \ll 1 \quad (14)$$

allows an effective simplification of the collision integral (13). Indeed, under condition (14), as collisions with fast electrons take place, the electrons in molecules can be regarded as free particles [10]. This means that the collision of high-energy electrons with molecules can be regarded as collisions with independent electrons and ions, i.e.,

$$F_m = F_e + F_i, \quad (15)$$

where F_i is the distribution function of ions and F_e is the distribution function of electrons in molecules. Then, in the first approximation with respect to the small parameter (14), the expression for the cross section q_{\pm} in the collision integral (13) is Coulomb-like and describes collisions of a high-energy electron (f) both with an atomic electron (F_e) and an ion (F_i).

The Coulomb cross section has a singularity at very small and very large scattering angles, which makes it possible (as is well known [26, 27]) to represent the collision integral in a differential form to a logarithmic accuracy. That is why, in the conditions considered, the collision integral St acquires the form [10, 24]

$$St(f) = \frac{1}{p^2} \frac{\partial}{\partial p} [p^2 (F_D + F_B) f(p, \mu)] + v(p) \frac{\partial}{\partial \mu} \left[(1 - \mu^2) \frac{\partial f(p, \mu)}{\partial \mu} \right]. \quad (16)$$

Here, p is the modulus of the electron momentum and μ is the cosine of the angle between the directions of the momentum \mathbf{p} and the electric field \mathbf{E} . The effective braking force $F = F_D + F_B$ describes the fast-electron energy loss due to ionization of molecules F_D (ionization loss) and generation of radiation F_B (bremsstrahlung loss):

$$F_D = \frac{4\pi e^4 N_m Z}{mc^2} \frac{\gamma^2}{\gamma^2 - 1} A, \quad Z = \sum_i n_i Z_i, \quad (17)$$

$$F_B = 4\alpha \frac{e^4 N_m Z \xi}{mc^2} (\gamma - 1) \left(\ln 2\gamma - \frac{1}{3} \right), \quad \xi = \sum_i \frac{n_i Z_i^2}{Z}.$$

Here, N_m is the molecular density, Z is the total number of electrons in a molecule (n_i is the number of atoms with charge Z_i in the molecule), γ is the Lorentz factor of the electron, $\varepsilon = mc^2(\gamma - 1)$ is its energy, and $A \approx \ln(\varepsilon/J_z)$ is the Bethe logarithm, $J_z = Ze_i$ [see (1)].

The effective frequency $v(p)$ of fast-electron scattering is mainly determined by its interaction with atomic nuclei:

$$v(p) = F_D \frac{\xi}{4\gamma p}. \quad (18)$$

Note that, although the force F_B is proportional to the small parameter α , as can be seen from (17), it increases effectively with γ and can become dominant for a high-energy electron.

3.3 Ionization integral

The main role in runaway breakdown is naturally played by ionization processes. At the same time, the number of high-energy electrons in the collision integral (16), (17) is readily seen to be conserved. That is why, to investigate the ionization effects, we have to make calculations with a higher accuracy than for the Landau integral. Ionization is the result of collisions between high-energy and atomic electrons. This process is fully described by the Boltzmann collision integral (13), where, according to (15), we should replace the distribution function F_m by F_e :

$$S(f, F_e) = \iint d\mathbf{v}_1 d\Omega u [q_-(u, \theta) f(\mathbf{v}) F_e(\mathbf{v}_1) - q_+(u, \theta) f(\mathbf{v}') F_e(\mathbf{v}_1')]. \quad (19)$$

As noted above, we do not need considering collisions between fast particles ($\propto ff$) because their number N_e is small compared to N_m . Atomic electrons do not collide at all.

The total Coulomb cross section $q(u, \theta)$ in (19) consists of three terms [28]:

$$q(u, \theta) = q^{(1)} - q^{(2)} + q^{(3)}, \quad (20)$$

which are specified by the following relations

$$q^{(1)} = \left(\frac{e^2}{mu^2} \right)^2 \frac{1}{\sin^4(\theta/2)},$$

$$q^{(2)} = \left(\frac{e^2}{mu^2} \right)^2 \frac{1}{\sin^2(\theta/2) \cos^2(\theta/2)}, \quad (21)$$

$$q^{(3)} = \left(\frac{e^2}{mu^2} \right)^2 \frac{1}{\cos^4(\theta/2)}.$$

Here, e and m are the electron charge and electron mass, and θ is the scattering angle. These terms formally appear in quantum-mechanical considerations because of the identity of particles, but they differ in physical meaning. The first term $q^{(1)}$ is the Rutherford cross section that describes the scattering of an incident high-energy electron, and the second term describes the exchange process in which an incident high-energy electron becomes a low-energy atomic electron and an atomic electron acquires a high energy. The third term reflects the arrival of newly born electrons. It is this third term in q_+ that is responsible for the ionization-induced increase in the number of fast electrons. We emphasize that the corresponding term responsible for the escape is absent. Indeed, such a process would correspond to the collision of two high-energy electrons with a low-energy electron produced. But in the processes of arrival this term is proportional to $F_m f$, while in the processes of escape it is proportional to f^2 , and, since $N_e \ll N_m$, we can discard it and consider the terms linear in f .

Thus, the arrival term q_+ and the escape term q_- can be represented as

$$q_+(u, \theta) = q^{(1)} - q^{(2)} + q^{(3)}, \quad q_-(u, \theta) = q^{(1)} - q^{(2)}. \quad (22)$$

The law of conservation of particles in the Boltzmann collision integral is obeyed provided that $q_- = q_+$. We can see that, in our case, this condition is not met; namely, the third term in (20), (21) is not balanced and describes the increase in the number of high-energy electrons.

The singular character of the Coulomb interaction cross section leads to the appearance of strong singularities in the kinetic equation (19). A special analysis is needed to remove these singularities correctly. In the next section, this will be done for the simplest case of a nonrelativistic, spherically symmetric distribution function. A general analysis of the 'elastic part' of the Boltzmann collision integral was carried out in Ref. [23], and the corresponding form of the total ionization integral will be given below without derivation.

3.4 Spherically symmetric distribution function

For simplicity, we consider a spherically symmetric distribution function $[f(\mathbf{v}) = f(v)]$ of fast electrons. In the first order with respect to the parameter (14), since the atomic electrons are low-energy ones, we represent their distribution function in the form of a delta function

$$F_e = N_m Z \delta(\mathbf{v}_1). \quad (23)$$

Here, Z is the total electric charge of atomic nuclei in molecules [see (17)]; therefore, $N_e = ZN_m$. Now we integrate the escape term in (19) over $d\mathbf{v}_1$ to obtain

$$S^- = \frac{8\pi Q}{v^3} f(v) \int \left(\frac{1}{\sin^3 \beta} - \frac{1}{\sin \beta \cos^2 \beta} \right) \cos \beta d\beta, \quad (24)$$

where the notation

$$Q = N_m Z \left(\frac{e^2}{m} \right)^2$$

is introduced for compactness. The term (24) has a singularity at $\beta \rightarrow 0$.

To cut off the singularity, let us analyze the arrival term. Since, according to (23), $F_e \propto \delta(\mathbf{v}'_1)$, this term can be rewritten as

$$S^+ = N_m Z \iint d\mathbf{v}_1 d\Omega u q_+(u, \theta) f(\mathbf{v}') \delta(\mathbf{v}' - \mathbf{v} - \mathbf{v}_1). \quad (25)$$

In the nonrelativistic case, the conservation laws have the form (for $\mathbf{v}'_1 = 0$)

$$\begin{aligned} \mathbf{v}' - \mathbf{v} - \mathbf{v}_1 &= 0, \\ v_1^2 + v^2 - v'^2 &= 0. \end{aligned} \quad (26)$$

The conservation laws (26) imply that the vectors \mathbf{v}' , \mathbf{v} , and \mathbf{v}_1 form a right-angled triangle. In view of this, after the integration of the delta function in equation (25) over $d\mathbf{v}_1$, the arrival term can be written as

$$\begin{aligned} S^+ &= \int d\Omega q_+ \left(\sqrt{v^2 + (\mathbf{v} - \mathbf{v}')^2}, \theta \right) \sqrt{v^2 + (\mathbf{v} - \mathbf{v}')^2} \\ &\quad \times f(v^2 + (\mathbf{v} - \mathbf{v}')^2). \end{aligned} \quad (27)$$

Elementary geometric constructions easily transform the integral (27) to the form

$$S^+ = 8\pi Q \int \sin \beta q_+ \left(\frac{v}{\cos \beta}, 2\beta \right) v f \left(\frac{v}{\cos \beta} \right) d\beta. \quad (28)$$

In view of (21), we find that the arrival term also has a singularity at $\beta \rightarrow 0$. Next, taking into account the normalization of the distribution function

$$4\pi \int f \left(\frac{v}{\cos \beta} \right) \left(\frac{v}{\cos \beta} \right)^2 d \left(\frac{v}{\cos \beta} \right) = N_e,$$

we represent the Boltzmann collision integral as

$$\begin{aligned} S &= S^+ - S^-, \\ S &= \frac{8\pi Q}{v^3} \int \frac{\cos \beta d\beta}{\sin^3 \beta} \left[\left(1 + \frac{\sin^4 \beta}{\cos^4 \beta} - \frac{\sin^2 \beta}{\cos^2 \beta} \right) f \left(\frac{v}{\cos \beta} \right) \right. \\ &\quad \left. - \left(1 - \frac{\sin^2 \beta}{\cos^2 \beta} \right) f(v) \right]. \end{aligned} \quad (29)$$

Thus, we can see that the strong singularities that were present in the original equation (29) are now canceled out. Only the logarithmic singularity remains that normally occurs in the Landau collision integral.

It is convenient to transform the integral obtained to a new form. To this end, we introduce the variable W instead of β :

$$\frac{\varepsilon}{W} = \cos^2 \beta. \quad (30)$$

Here, ε is the kinetic energy of the fast electron and W is its energy before the collision. In the new variables (30), the

Boltzmann collision integral (29) becomes

$$\begin{aligned} S &= S^+ - S^-, \\ S^+ &= \frac{4\pi Q}{\sqrt{m\varepsilon}} \int_{\varepsilon}^{\infty} \left\{ \left[\frac{1}{\varepsilon^2} + \frac{1}{(W - \varepsilon)^2} - \frac{1}{\varepsilon(W - \varepsilon)} \right] F(W) \right\} dW, \\ S^- &= \frac{4\pi Q}{\sqrt{m\varepsilon}} \int_{\varepsilon}^{\infty} \left\{ \left[\frac{1}{(W - \varepsilon)^2} - \frac{1}{\varepsilon(W - \varepsilon)} \right] F(\varepsilon) \right\} dW. \end{aligned} \quad (31)$$

The arrival term S^+ is analogous to the well-known Möller formula that describes both the ionization (the first term) and the scattering of electrons [29].

We single out the ionization term to obtain

$$\begin{aligned} S &= St + S_I, \\ St &= \frac{4\pi Q}{\sqrt{m\varepsilon}} \int_{\varepsilon}^{\infty} \left[\frac{1}{(W - \varepsilon)^2} - \frac{1}{\varepsilon(W - \varepsilon)} \right] [F(W) - F(\varepsilon)] dW, \\ S_I &= \frac{4\pi Q}{m^{1/2}\varepsilon^{5/2}} \int_{\varepsilon}^{\infty} F(W) dW. \end{aligned} \quad (32)$$

After the integration by parts, the scattering integral St can be rewritten as

$$\begin{aligned} St &= \frac{4\pi Q}{\sqrt{m\varepsilon}} \tilde{A} \frac{dF}{d\varepsilon} \\ &\quad + \frac{4\pi Q}{\sqrt{m\varepsilon}} \int_{\varepsilon}^{\infty} \left\{ \frac{W}{\varepsilon} \left[\ln \left(\frac{W}{\varepsilon} - 1 \right) - 1 \right] + 1 \right\} \frac{d^2 F}{dW^2} dW. \end{aligned} \quad (33)$$

Here \tilde{A} is the Coulomb logarithm. The first right-hand term in (33) is the friction force of a high-energy electron in a gas. The integral term in (33) is not divergent and has a slow logarithmic function in the integrand. As usually, we neglect this slow variation in the integration in (33) assuming $\ln(\dots) \approx \text{const}$. This integration implies a renormalization of the logarithm. Upon substituting the renormalized logarithm A for \tilde{A} in (33), we finally obtain the Boltzmann collision integral for a spherically symmetric function in the form

$$S = \frac{4\pi Q}{\sqrt{m\varepsilon}} A \frac{dF}{d\varepsilon} + \frac{4\pi Q}{m^{1/2}\varepsilon^{5/2}} \int_{\varepsilon}^{\infty} F(W) dW. \quad (34)$$

Here the first right-hand term completely takes into account the energy loss by fast electrons and the second, the ionization-induced increase in their number. One can see that the first term proportional to the Coulomb logarithm A is the leading one. The second (ionization) term is a nonlogarithmic correction to the Landau integral.

3.5 The general form of the ionization integral

We shall now present the general form of the relativistic ionization integral [23]:

$$\begin{aligned} S_I &= N_m v \frac{2\pi Z e^4}{mc^2} \int_{\varepsilon}^{\infty} \frac{\gamma'^2}{\gamma^2 - 1} \left[\frac{1}{\varepsilon^2} + \frac{1}{(W + mc^2)^2} \right] \times \\ &\quad \times \int \frac{d\phi}{2\pi} F(W, \mu', \phi) \delta(\mu_1 - \mu_0) d\mu_1 dW, \\ \mu' &= \frac{\mu\mu_1 \pm (1 - \mu_1^2)^{1/2} \sin \phi \sqrt{\mu_1^2 - \mu^2 + (1 - \mu_1^2) \sin^2 \phi}}{\mu_1^2 + (1 - \mu_1^2) \sin^2 \phi}, \\ \mu_0 &= \left[\frac{\varepsilon(W + 2mc^2)}{W(\varepsilon + 2mc^2)} \right]^{1/2}; \quad \gamma' = 1 + \frac{W}{mc^2}. \end{aligned} \quad (35)$$

Here, μ is the cosine of the polar angle, ϕ is the azimuthal angle between the direction of the electron momentum \mathbf{p}' before the collisions and the direction of the electric field \mathbf{E} , the term $\delta(\mu_1 - \mu_0)$ expresses the momentum conservation law, and $\varepsilon = mc^2(\gamma - 1)$ is the kinetic energy of the electron. In the nonrelativistic limit the integral (35) can be substantially simplified:

$$S_I = \frac{Q}{2\varepsilon^{5/2}} \int_{\varepsilon}^{\infty} dw \times \int_0^{2\pi} f\left(w, \mu \sqrt{\frac{\varepsilon}{w}} + \sqrt{1 - \mu^2} \sqrt{1 - \frac{\varepsilon}{w}} \cos \phi\right) \frac{d\phi}{2\pi}. \quad (36)$$

Note that, when integrating expression (36) over the angle $d\phi$, it is convenient to employ the Legendre polynomial expansion of the distribution function of fast electrons $f(\mathbf{v})$ [$v = |\mathbf{v}| = \sqrt{(2\varepsilon/m)}$]:

$$f(v, \mu) = \sum_{j=0}^{\infty} f_j(v) P_j(\mu). \quad (37)$$

Applying the summation theorem for Legendre polynomials, after integration over $d\phi$, we obtain

$$S_I = \frac{Q}{v^3} \sum_{j=0}^{\infty} \int_0^1 f_j\left(\frac{v}{\tau}\right) P_j(\tau) \frac{d\tau}{\tau^3} P_j(\mu). \quad (38)$$

In other words, the ionization integral can be represented by a Legendre polynomial expansion into independent components S_{Ij} .

4. Runaway breakdown (kinetic theory)

4.1 Statement of the problem

In the kinetic theory, the problem of runaway breakdown is formulated as follows. Fast electrons in matter, described by the kinetic equation (11), are considered. In a simple statement, the electric field E , the density N_m of neutrals and their charge Z can be assumed to be constant. In this case, a homogeneous solution to equation (11), independent of spatial coordinates, is considered, i.e., the kinetic equation (11) is solved only in the momentum space (\mathbf{p}) or in the energy (ε) and angular-momentum (μ) space. This particular statement of the problem will be considered below, except in the last two sections.

The boundary condition at high energies ($\gamma \rightarrow \infty$) is obvious: $f = 0$. In the region of relatively low, nonrelativistic energies $\varepsilon \ll \varepsilon_c$, a natural condition is a free particle outflow to low energies. It is this condition that determines the runaway breakdown for which the processes in the low-energy range $\varepsilon \leq \varepsilon_i$ are not important.

In view of the linearity of the kinetic equation, its solution in a homogeneous medium under the indicated boundary conditions can asymptotically be exponential in time and no other:

$$f \propto \exp(\lambda t). \quad (39)$$

The runaway breakdown will then be realized only if $\lambda > 0$ for all eigenvalues. The proof of the existence of a solution with positive λ values and the evaluation of this parameter or the time $\tau = 1/\lambda$ of the exponential growth of the number of runaway electrons (and the characteristic avalanche growth

length $l_a = c/\lambda$) and other parameters are the main problems of the breakdown theory.

An important specific feature of runaway breakdown is the necessity of the existence of high-energy seed particles. In the kinetic language this means that both the very possibility of breakdown and its parameters may depend on the form of the initial distribution function of electrons. The investigation of this RB feature is among the principal problems of kinetic theory.

4.2 The structure of the distribution function

The variation of the friction force $F = F_D + F_B$ acting on a fast electron is shown in Fig. 2 with allowance for the ionization and bremsstrahlung losses. It can be seen that, as in the elementary theory, the runaway of electrons is possible in a constant electric field for $E > E_c$ (3). In this case, for low energies ($\varepsilon < mc^2$) the boundary of the runaway region is, as before, determined by the ionization loss (1) ($F = F_D$) and for higher electron energies by the bremsstrahlung loss (17) ($F = F_B$) with much weaker ionization losses. Hence, it is the bremsstrahlung loss (neglected in the elementary theory) that in fact determines the size $\Delta\varepsilon_r$ of the runaway region:

$$\Delta\varepsilon_r = \varepsilon_{c2} - \varepsilon_c \approx mc^2 \frac{\pi a}{\alpha Z \ln(2\gamma)} \frac{E}{E_c}. \quad (40)$$

We can see that the highest energy ε_{c2} of runaway electrons increases nearly linearly with increasing E/E_c because $\varepsilon_{c2} \gg \varepsilon_c$. For instance, in air it reaches 430 MeV at $E/E_c = 5$ and 850 MeV at $E/E_c = 10$.

In the theory of runaway electrons in a fully ionized plasma, the main reservoir that supplies electrons to the runaway region is a large mass of thermal plasma [10]. No such mass exists in the runaway breakdown theory, in which electrons themselves are generated owing to ionization processes. Therefore, a decisive influence on both the very possibility of breakdown and the structure of the distribution function is exerted by the ionization integral (35).

Numerical solutions to the kinetic equation (11) have been obtained in Refs [17–24]. The moderate-energy range $\gamma \leq Z/2$ stands out, where an important role is played by the scattering by atomic nuclei described in (16) by the term proportional to the scattering frequency $\nu(p)$. In this region,

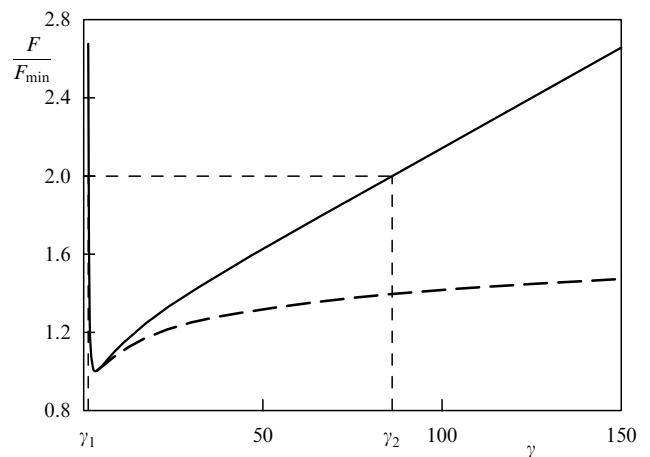


Figure 2. Friction force F normalized to F_{\min} as a function of the relativistic electron energy $\gamma = \varepsilon/mc^2 + 1$. The dashed line shows this dependence with allowance for the ionization loss only; γ_1 and γ_2 are the boundaries of the runaway region (40).

the distribution function is two-dimensional in the space of energy γ and angular momentum μ . For high values $\gamma > Z/2$, the scattering by nuclei becomes insignificant because the scattering frequency $\nu(p)$ falls as $1/\gamma$ (18). In this region, the spread in μ is not large, and therefore high-energy electrons move, in fact, along the field ($\mu \simeq 1$) [24].

Examples of numerical solutions to the kinetic equation are presented in Figs 3 and 4. Figure 3 shows that, for low energies, the width of the angular distribution is appreciable. For instance, at $\varepsilon = 0.1$ MeV, the function falls by 10% from the direction of the electric field $\theta = 0$ ($\mu = 1$) to an angle of $\theta = 50^\circ$ ($\mu = 0.672$) and decreases 1.6 times to an angle of $\theta = 90^\circ$ ($\mu = 0$). Only in the opposite direction ($\mu = -1$), the decrease of f becomes large, reaching 5.3 times. As the energy rises, the directivity increases considerably: for $\varepsilon = 1$ MeV, the distribution function decreases 2.5 times from $\theta = 0$ to $\theta = 50^\circ$ and 9 times to the perpendicular direction ($\theta = 90^\circ$). For an energy of 5 MeV, the directivity is already very high. Thus, in full accordance with the above qualitative analysis, the numerical solution demonstrates a strong directivity of the distribution function along the electric field in the region of high electron energies. As γ increases, it falls exponentially and vanishes in any case near the runaway boundary at high energies ε_2 , i.e., near the second point of intersection of eE with F (see Fig. 2). In the low-energy range, the distribution function grows effectively with falling ε :

$$f \sim \varepsilon^{-1}. \quad (41)$$

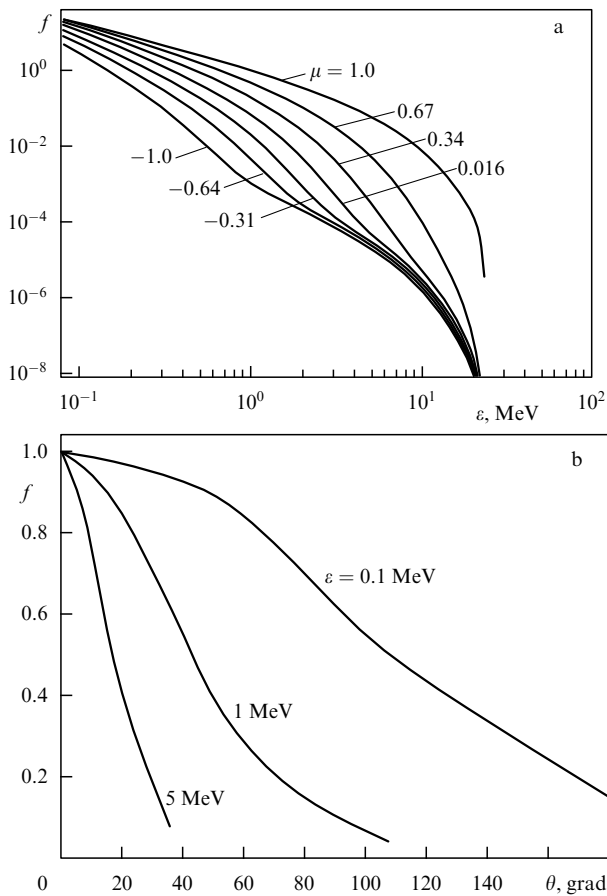


Figure 3. Dependence of the distribution function f for $E/E_c = 2$ (a) on the electron energy ε for different values of the angular momentum μ and (b) on the angle $\theta = \arccos \mu$ for different values of the energy ε .

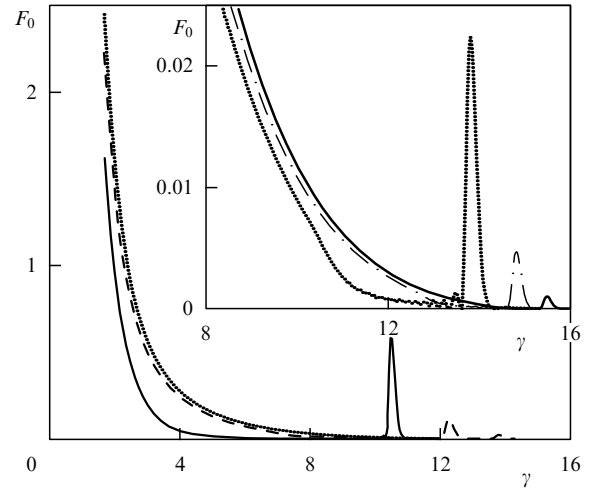


Figure 4. Pre-exponential function F_0 for $E/E_c = 1.21$ and $\gamma_0 = 10$ at different instants of time t : light solid line, $t = 5.6$; dashed line, $t = 28$; dotted line, $t = 84$; dash-and-dot line, $t = 84$; heavy solid line, $t = 112$ [the time t is normalized to t_0 (45)].

The influence of the initial distribution on the development of the solution was investigated numerically in Ref. [24], where the initial function f_0 was chosen in the form of a narrow seed beam near a given energy ε_0 . If the energy is $\varepsilon_0 < \varepsilon_c$, the solution of the kinetic equation (11) with a positive λ (39) is absent whatever the strength of the electric field. In other words, runaway breakdown is not realized in this case. This fully corresponds to the elementary theory: for a runaway breakdown to be realized, seed electrons of energies $\varepsilon > \varepsilon_c$ are necessary.

If $\varepsilon_0 > \varepsilon_c$, a breakdown occurs, and the function $f(\gamma, t)$ for large t grows exponentially with time:

$$f(\gamma, t) = F_0(\gamma) \exp(\lambda t). \quad (42)$$

It is of importance that the exponent λ is virtually independent of F_0 and of the energy ε_0 of the initial beam. Thus, provided that $\varepsilon_0 > \varepsilon_c$, the initial form of the distribution function virtually does not affect the character of its exponential growth or the increase of the number of fast electrons (Fig. 5).

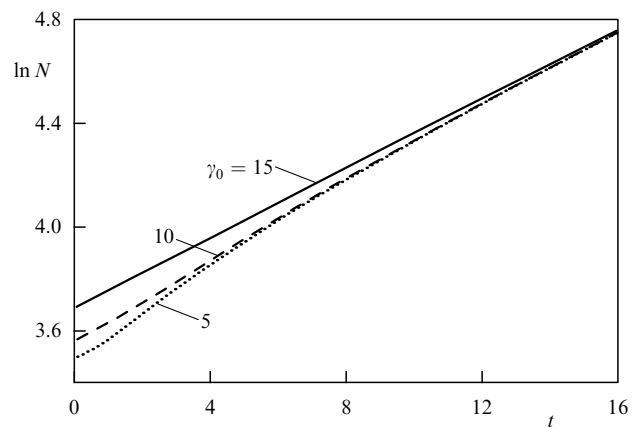


Figure 5. Runaway electron density N as a function of time t for various energies γ_0 of the initial beam. The time t is normalized to t_0 and the density N to the initial electron density N_0 in the beam. At the initial moment, for any γ_0 , the increase of N is extremely sharp and is associated with the generation of slow electrons (41).

It can also be seen from Fig. 4 that the electron energy in the seed beam increases with time. This is natural, since the runaway electrons are accelerated by the field. At the same time, the *relative magnitude* of the seed part of the distribution function decreases exponentially with time. This is due to the fact that, in the course of the breakdown, it is only the eigenfunction of the solution corresponding to the maximum eigenvalue λ of the kinetic equation (11) that grows exponentially with time. As a result, the solution $F_0(\gamma)$ established asymptotically as is completely independent of the initial distribution function if the condition $\lambda > 0$ is met.

4.3 The time of exponential growth

The time of the exponential growth of the solution, $\tau = 1/\lambda$, depends essentially on the magnitude of the electric field. It decreases with increasing E/E_c approximately as $(E_c/E)^{3/2}$. The results of the numerical calculations of the quantity λ [18–21, 24] are summarized in Fig. 6, where the approximate dependence obtained in the analytical theory is also presented [see (53) below]. Note that Fig. 6 shows only a solution to the kinetic equation (11). The results of Monte Carlo calculations yield somewhat different numerical values of λ [21]; the reason for this difference is not yet clear.

The solid line in Fig. 6 describes the characteristic parameter of the avalanche of runaway electrons, l_a , determined according to the ‘elementary’ theory (9). We can see that the ‘elementary’ theory is in reasonable agreement with the exact kinetic calculation. The reason is that the main role in the breakdown is played by electrons with energies close to ε_c .

We emphasize that the parameter λ turns out to be negative ($\lambda \leq 0$), that is, *the runaway breakdown does not occur* in the cases where

(1) the electric field E is not sufficiently strong, i.e., $E < E_c$;

(2) there are no fast seed electrons with energies $\varepsilon_0 > \varepsilon_c$;

(3) the distribution function $f(v, \mu)$ of electrons is close to a spherically symmetric function f_0 , i.e., it differs from f_0 only by the first Legendre polynomial (37):

$$f(v, \mu) = f_0(v) + \mu f_1(v). \quad (43)$$

This case embraces, for example, breakdown in an alternating electric field or in a constant electric field perpendicular to a magnetic field $\mathbf{E} \perp \mathbf{B}$ (for $B \gg E$).

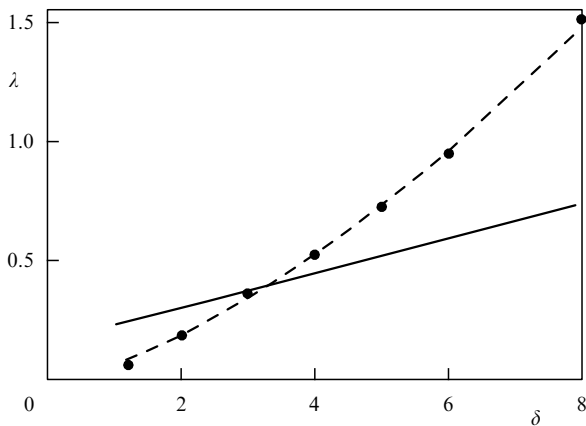


Figure 6. Dependence of λ on $\delta = E/E_c$: the points show the results of numerical calculations, the dashed line is the analytical curve (53), and the solid line represents the elementary theory (9) [λ is expressed in $1/t_0$ (45)].

As is well known, normal breakdown can be realized in all these cases; it is quite analogous to breakdown in a constant electric field and has a critical field E_{th} close in magnitude [30, 31]. This is not the case with runaway breakdown. Our numerical and analytical analyses have shown that, whenever the distribution function is close to a spherically symmetric one (43), the asymptotic solution of the kinetic equation (11) has no positive roots λ . This feature, i.e., the necessity of a constant electric field that brings about a noticeable asymmetry in the distribution function at $\varepsilon > \varepsilon_c$ for RB occurrence, also substantially distinguishes runaway breakdown from other mechanisms of electrical breakdown of matter.

4.4 Analysis of the asymptotic behavior of the distribution function

The above considerations mainly concerned the results of numerical calculations. In this section, we analyze the asymptotic behavior of the solution of the kinetic equation (11). It is natural to begin with an examination of the range of moderate electron energies, where the dominant role is played by the ionization losses:

$$\gamma \ln^2(2\gamma) \ll \frac{\pi}{\alpha Z} \ln^2\left(\frac{mc^2}{J_z}\right). \quad (44)$$

For this region, it is convenient to introduce the dimensional variables

$$u = \frac{v}{c}, \quad \delta = \frac{E}{E_c}, \quad t_1 = \frac{t}{t_0}, \quad (45)$$

where

$$E_c = \frac{4\pi Ze^3 N_m}{mc^2} A, \quad t_0 = \frac{m^2 c^3}{4\pi e^4 Z N_m A}.$$

As noted above, from the mathematical point of view, the breakdown phenomenon implies that the asymptotic form of the distribution function is (39)

$$f(u, \mu, t_1) = f(u, \mu) \exp(\lambda t_1), \quad (46)$$

and we have to find the maximum positive eigenvalue λ of the linear equation

$$\begin{aligned} \lambda f + \delta \left\{ \mu \frac{\partial f}{\partial u} + \frac{1-\mu^2}{u} \frac{\partial f}{\partial \mu} \right\} &= \frac{1}{u^2} \frac{\partial f}{\partial u} + \frac{\xi}{u^3} \frac{\partial}{\partial \mu} \left\{ (1-\mu^2) \frac{\partial f}{\partial \mu} \right\} \\ &+ \frac{1}{Au^3} \sum_{j=0}^{\infty} \int_0^1 f_j\left(\frac{u}{\tau}\right) P_j(\tau) P_j(\mu) \frac{d\tau}{\tau^3}. \end{aligned} \quad (47)$$

Here, the expansion (38) for the ionization integral in a nonrelativistic region is taken into account.

A simple representation of the ionization integral in the form (38) allows one to seek the solution in the form of a Legendre polynomial expansion. From (37) and (47), we obtain the following system of coupled equations:

$$\begin{aligned} \delta \left\{ \frac{j}{2j-1} u^{j-1} \frac{d}{du} (u^{1-j} f_{j-1}) + \frac{j+1}{2j+3} u^{-j-2} \frac{d}{du} (u^{j+2} f_{j+1}) \right\} \\ = -\lambda f_j - \frac{1}{u^2} \frac{df_j}{du} - \frac{\xi}{u^3} j(j+1) f_j + \frac{1}{Au^3} \int_0^1 f_j\left(\frac{u}{\tau}\right) P_j(\tau) \frac{d\tau}{\tau^3}. \end{aligned} \quad (48)$$

For low particle velocities ($u^2\delta \ll 1$), equation (48) implies that

$$f_0 \propto u^{-2-1/A}, \quad f_1 \propto u^{-1-1/[A(2\xi-1)]} \dots, \\ f_2 \sim f_4 \sim \dots \sim f_0, \quad f_3 \sim f_5 \sim \dots \sim f_1.$$

This indicates that even for low velocities u the distribution function is essentially anisotropic. Indeed, $f_2 \sim f_4 \sim \dots \sim f_0$, although $f_1 \ll f_0$. This corresponds to the results of numerical calculations (see Fig. 3). The anisotropy is generated by the ionization integral.

We shall now consider the solution of system (48) for high velocities ($u^2\delta \gg 1$). We can make certain that, in this approximation, the leading term for each polynomial f_j has the form

$$f_j \approx \frac{2j+1}{2} \exp\left(-\frac{\lambda}{\delta} u\right).$$

This structure of the coefficients of Legendre polynomial expansion suggests that the distribution function tends to a delta function. Indeed,

$$f(u, \mu) = \sum_{j=0}^{\infty} f_j(u) P_j(\mu) \approx \sum_{j=0}^{\infty} \frac{2j+1}{2} P_j(\mu) \exp\left(-\frac{\lambda}{\delta} u\right) \\ = \exp\left(-\frac{\lambda}{\delta} u\right) \delta(\mu - 1). \quad (49)$$

Thus, we can see that, with increasing particle energy, the distribution function becomes strongly directed (see Fig. 3). Furthermore, in spite of the fact that in the nonrelativistic statement of the problem the electron energy increases unlimitedly under the condition $\varepsilon > \varepsilon_c$, i.e., $u^2 > 1/\delta$, the distribution function (49) that is established at $\lambda > 0$ falls exponentially (see Fig. 4). Physically, this can be explained by the fact that, with increasing energy, the efficiency of particle production weakens according to (34), (35). That is why the appearance of particles at high velocities is only due to the increase of their energy under the effect of the electric field. The latter process is proportional to the time ($v = eEt/m$), but, since the distribution function itself increases exponentially in time (46), the time-independent pre-exponential term in (46) turns out to be $\exp(-\lambda t_0)$, where λ^{-1} is the time of increase in the number of particles and $t_0 = mv/eE = u/\delta$ is the acceleration time. Recall that we are considering here a nonrelativistic theory ($u^2 < 1$) under the condition $u^2\delta \gg 1$. This holds only in the case of a strong electric field ($\delta \gg 1$).

We will see below that $\lambda \propto \delta^{3/2}$ [see (53)]. Therefore, according to (49), for strong electric fields ($\delta \gg 1$), the distribution function falls sharply at high energies ($u^2\delta \gg 1$). This fact suggests that the number of particles with high relativistic energies is relatively small. Hence, even a nonrelativistic theory can describe the runaway breakdown phenomenon with a fairly good accuracy.

We now determine the rate of the exponential growth of the distribution function in time. We take into account the fact that the main role in the runaway breakdown for $\delta \gg 1$ is played by the moderate-energy range $\varepsilon \sim \varepsilon_c \sim 1/\delta$. This makes it possible to simplify the collision integral and, upon integrating equation (11) over the angular variable μ , to

represent it as

$$\frac{\partial f_0}{\partial t} + \delta \frac{1}{u^2} \frac{\partial}{\partial u} (u^2 f_0) = \frac{1}{u^2} \frac{\partial f_0}{\partial u} + \frac{1}{au^5} \int_u^{\infty} f_0(k) k dk, \\ f_0 = \frac{1}{2} \int_{-1}^1 f(\mu, u) d\mu. \quad (50)$$

Equation (50) possesses an important quantity: we can eliminate the parameter of the electric field δ from it. Indeed, introducing the new variables

$$\tau = 2\delta^{3/2} t, \quad y = u^2 \delta^2, \quad \Phi = \exp\left(\frac{2\sigma\tau}{a}\right) \int_{\sqrt{y/\delta}}^{\infty} f_0(k) k dk,$$

we bring equation (50) into the form

$$(1-y)\Phi'' - \left(\frac{\sigma}{a} \sqrt{y} + 1\right) \Phi' - \frac{\Phi}{4ay^2} = 0. \quad (51)$$

Next, taking into account that $a \gg 1$ and using the technique of matched asymptotic expansions in $1/a$, we determine implicitly the eigenvalue σ of the problem:

$$\sigma \ln\left(\frac{a^3}{16\sigma^2}\right) = \frac{1}{2} \ln\left[\frac{a}{2} \left(1 + \frac{2}{a} + \sqrt{1 + \frac{4}{a}}\right)\right] \\ + \left(1 + \frac{4}{a}\right)^{-1/2} + O\left(\frac{\sigma}{a}\right). \quad (52)$$

It follows herefrom that, to a logarithmic accuracy, the growth rate is

$$\lambda \approx \frac{0.6}{a} \delta^{3/2}. \quad (53)$$

To put it differently, the time $\tau = 1/\lambda$ of the exponential growth in dimensional variables is equal to [24]

$$\tau = \frac{m^2 c^3}{1.4\pi e^4 N_m Z} \left(\frac{E_c}{E}\right)^{3/2}. \quad (54)$$

This value agrees well with the numerical results and with the characteristic avalanche length $l_a = c\tau$ obtained from the elementary theory (see Fig. 6).

4.5 Spatially nonuniform breakdown

It has been assumed above that both the electric field E and the flux of fast seed electrons are uniform in space. At the same time, high-energy seed electrons may be rare. In this case, the latter condition is not met. We will now therefore consider how a runaway breakdown generated by a single fast seed electron develops. Let \mathbf{s} be the direction of motion of a fast electron coincident with the direction of the electric field \mathbf{E} . Given this, the runaway breakdown develops not only in the \mathbf{s} direction, but also in the orthogonal plane \mathbf{r} . In the approximation of elementary theory, the process can be described by the diffusion equation [16]

$$\frac{\partial N}{\partial s} = \frac{1}{l_a} N(s - s_0) + \frac{1}{r} \frac{\partial}{\partial r} \left(D r \frac{\partial N}{\partial r} \right). \quad (55)$$

Here, $N(s, r)$ is the number of fast electrons, l_a is the characteristic avalanche length, s_0 is the distance over which an electron gains the energy necessary for the generation of a new runaway electron, and D is the transverse diffusion

coefficient. Diffusion is controlled by both the scattering of fast electrons by molecular nuclei and the velocity spread of newly generated electrons. Note that this problem was solved not only in elementary theory but also in kinetic theory by the Monte Carlo method [22]. The results of the calculations proved to be fairly close.

The solution of equation (55) with the initial condition

$$N_{s=0} = N_0 \delta(\mathbf{r}_\perp)$$

has the form

$$N(s, r) = \frac{N_0}{4\pi s D} \exp\left(\frac{s - s_0}{l_a} - \frac{r^2}{4Ds}\right). \quad (56)$$

This demonstrates that the discharge spreads in the plane orthogonal to the direction of the electric field and always remains inside a cone with an angle of $\theta_c = 2\sqrt{D/l_a}$:

$$r \leq r_c = 2\sqrt{\frac{D}{l_a}} s, \quad \theta < \theta_c = 2\sqrt{\frac{D}{l_a}}.$$

The cone is narrow and becomes narrower with increasing field.

The spatial distribution of runaway-electron density is plotted in Fig. 7. The figure demonstrates that, near the asymptote θ_c (shown by the dashed line), the density gradient increases sharply. At the same time, near the discharge axis, $N(s, r)$ decreases only slightly compared to the exponentially growing avalanche in a uniform flux.

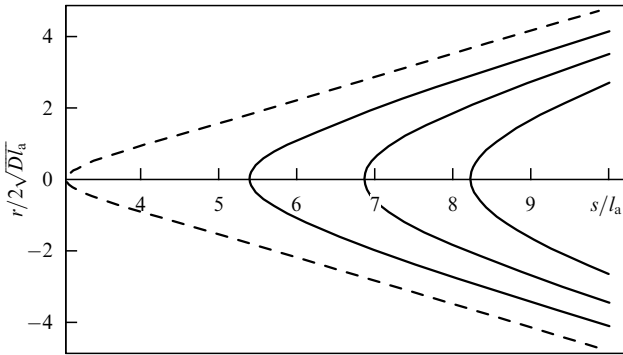


Figure 7. Contours of runaway-electron density.

4.6 Runaway avalanches in a nonuniform electric field

We have considered above the runaway breakdown in a uniform electric field. In a nonuniform field $\mathbf{E}(\mathbf{r})$ the picture is much more complicated, and the solution to the complete kinetic equation should be analyzed. For simplicity, we assume the electric field to vary in space only in magnitude but not in direction, i.e., $E = E(z)$. Then equation (11) can be written as

$$\begin{aligned} v\mu \frac{\partial f}{\partial z} + \frac{e}{m} E(z) \left(\mu \frac{\partial f}{\partial v} + \frac{1 - \mu^2}{v} \frac{\partial f}{\partial \mu} \right) \\ = \frac{1}{v^2} \frac{\partial}{\partial v} (v^2 F_D f) + \frac{v}{v^3} \frac{\partial}{\partial \mu} \left((1 - \mu^2) \frac{\partial f}{\partial \mu} \right) + S_I. \end{aligned} \quad (57)$$

We consider here not very high electron energies, in which case the force F_B can be neglected to a first approximation.

A runaway breakdown occurs if $E > E_c$ and the scale of the field nonuniformity L exceeds the characteristic avalanche length l_a . Moreover, seed electrons with energies $\varepsilon > \varepsilon_c$ (4) are necessary. We assume the intensity of the source of seed electrons, $q = q(\gamma)$, to be constant and the electric field of strength $E \sim E_c$ to be localized in space:

$$E = E_{\max} \left(1 - \frac{z^2}{L^2} \right), \quad -L \leq z \leq L. \quad (58)$$

This means that the breakdown is also localized in the region $E \sim E_c$, i.e., it is a locally growing avalanche of runaway electrons. In a uniform field, a rather good approximation is that of a distribution function strongly directed along the electric field. That is why, upon integrating equation (57) over the angle μ , we arrive at the following stationary equation for the distribution function $f(\gamma, \mu)$ of fast electrons:

$$(\gamma^2 - 1) \frac{\partial f}{\partial z} = \frac{\partial}{\partial \gamma} \{ (\gamma^2 - 1) [\Phi_D - E(z)] f \} + S_I + q(\gamma). \quad (59)$$

We use here the dimensionless variables substituting $z \rightarrow z/l_a$, where l_a is the characteristic length of the runaway avalanche (Φ_D is the friction force accordingly normalized), and the electric field is

$$E(z) = \delta(1 - a_l^2 z^2),$$

where $\delta = E/E_c$, $a_l = l_a/L$. Then, as follows from (35), the ionization integral is determined by the simple expression

$$S_I = \frac{1}{2} \int_1^\infty y^2 f(y, z) \left[\frac{1}{(\gamma - 1)^2} + \frac{1}{y^2} \right] dy.$$

The initial function $f_0(\gamma)$ in equation (59) is determined by the action of the source $q(\gamma)$, i.e., is a solution to the equation in the absence of the electric field $E(z)$. The same function serves as a boundary condition for $z = -1/a_l = -L/l_a$. The natural boundary condition in the energy space is $f(\gamma, z) \rightarrow 0$ as $\gamma \rightarrow \infty$.

Solutions of equation (59) are plotted in Figs 8 and 9. The former presents the dependence of the distribution function

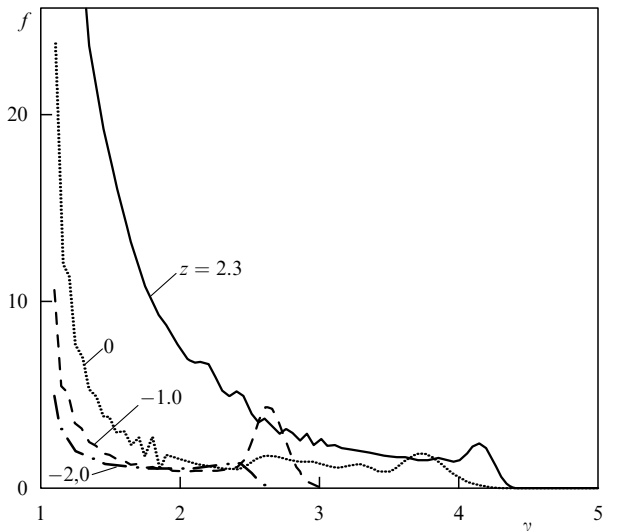


Figure 8. Energy dependence of the distribution function at various altitudes z for $E_{\max}/E_c = 1.1$.

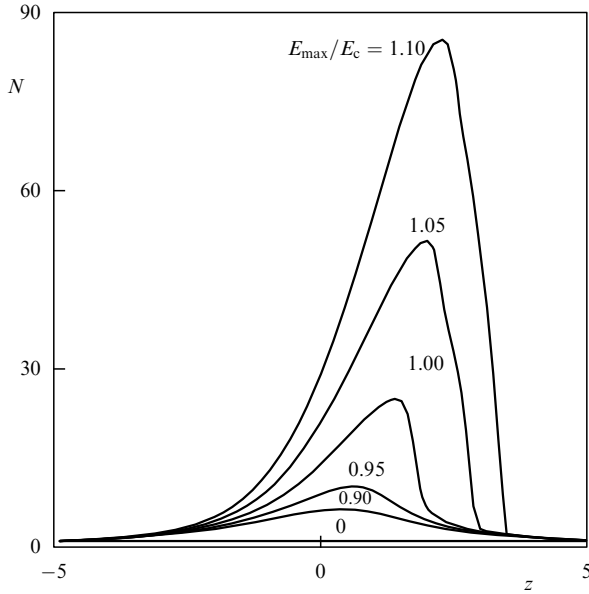


Figure 9. Altitude dependence of the runaway-electron density N normalized to the density $q(\gamma)$ produced by the source.

on the energy γ at various altitudes z . Its general form is similar to that considered in the case of a uniform field. Figure 9 shows that the increase of the electric field, starting from the point $z = -5$ (the parameter a_l is taken equal to 0.2), is accompanied by a rapid growth in the distribution function $f(\gamma)$. Accordingly, the total number N of fast electrons increases (see Fig. 9). At the point $z = 0$ the field reaches its maximum. The maximum of $N(z)$ is reached at the point $z = 2.3$ somewhat displaced in the direction of the electron motion. The displacement increases with increasing field maximum $\delta = E_{\max}/E_c$. For $E_{\max}/E_c > 1$, one can clearly see an avalanche-like growth in the number of fast electrons. A sharp avalanche cut-off starts beyond the point at which $E(z)$ becomes smaller than E_c . The maximum density N_{\max} of fast electrons, reached in an avalanche, grows exponentially with increasing field E_{\max}/E_c . At the same time, the point z_{\max} at which $N(z)$ reaches its maximum shifts rather smoothly with increasing E_{\max}/E_c . For example, for $E_{\max}/E_c = 1.2$ we have $z_{\max}/l_a = 2.6$.

On the whole, we can say that the number of fast electrons in a nonuniform electric field increases in space as an avalanche (i.e., exponentially sharply) in the range of $E(z)$ values exceeding E_c . If the maximum electric-field strength E_{\max} does not reach E_c , such a growth is not observed. All these specific features typical of runaway breakdown in a nonuniform field manifest themselves only for sufficiently large spatial scales $L \gg l_a$ of the nonuniformity region.

5. Conditions for the occurrence of runaway breakdown in the atmosphere

As follows from the theory presented above, runaway breakdown can occur provided that

- (1) the electric field strength E exceeds the critical value E_c (3):

$$E \geq E_c; \quad (60)$$

- (2) the spatial scale L on which condition (60) holds substantially exceeds the length l_a (9) of the exponential

growth of the avalanche:

$$L \gg l_a; \quad (61)$$

- (3) fast seed electrons with energies

$$\varepsilon > \varepsilon_c = \frac{mc^2 E_c}{2E} \quad (62)$$

are present.

The most interesting among the presently known manifestations of RB are observed in the thunderstorm atmosphere. We dwell on the main conditions for the occurrence of this effect in the atmosphere.

The critical RB field in the atmosphere (3) is

$$E_c = 2.16 \frac{\text{kV}}{\text{cm}} \times P = 216 \exp\left(-\frac{z}{h}\right) \frac{\text{kV}}{\text{m}}. \quad (63)$$

Here, P is the air pressure (in atmospheres), z is the altitude above sea level, and $h \simeq 8$ is the scale height of the atmosphere. As noted in Section 3, the field E_c is an order of magnitude lower than the threshold field of normal breakdown

$$E_{\text{th}} \simeq 23 \frac{\text{kV}}{\text{cm}} \times P.$$

As follows from (63), the critical field E_c falls exponentially with altitude z . For example, at an altitude of $z \approx 6.3$ km, the critical field is $E_c = 100 \text{ kV m}^{-1}$ and at an altitude of $z \approx 11$ km, $E_c = 50 \text{ kV m}^{-1}$.

In thunderclouds the scale condition (61) is typically fulfilled fairly well. Fast seed particles are here secondary cosmic-ray electrons, whose mean flux density at altitudes of 4–8 km is comparatively high [32–34]:

$$\Phi \simeq 10^3 \text{ m}^{-2} \text{ s}^{-1}. \quad (64)$$

Thus, as soon as the electric field E in a thundercloud reaches the value E_c (63), the RB process can develop. Since secondary cosmic-ray electrons have energies of up to 30 MeV and move in all directions due to scattering by nuclei, the breakdown can develop in any direction, either down to the Earth or up to the ionosphere, depending on the sign of the electric field. The main role is played here by the possibility of the appearance of the necessary electric field, which depends on the relation between the processes of generation and relaxation of the field E .

The relaxation is determined by the air conductivity:

$$\tau_r = (4\pi\sigma)^{-1}. \quad (65)$$

Here, τ_r is the relaxation time and σ is the air conductivity. This is the ion conductivity, since free thermal electrons in air become attached to molecules very rapidly (within less than 10^{-7} s). The conductivity depends on the ionization produced by cosmic rays [32, 35, 36] and on the ion collision frequency, which falls exponentially with altitude because of the variation in the atmospheric density. Near the Earth's surface the relaxation time is $\tau_r \simeq 400$ s [35]. The variation of the relaxation time with altitude is shown in Fig. 10. At an altitude of 10 km, $\tau_r \sim 100$ s and at 30–50 km, it falls to 1–10 s. We emphasize that inside clouds the conductivity can fall appreciably [35], i.e., the relaxation time can increase, because of the trapping of some share of free ions by aerosols, water droplets, and ice particles.

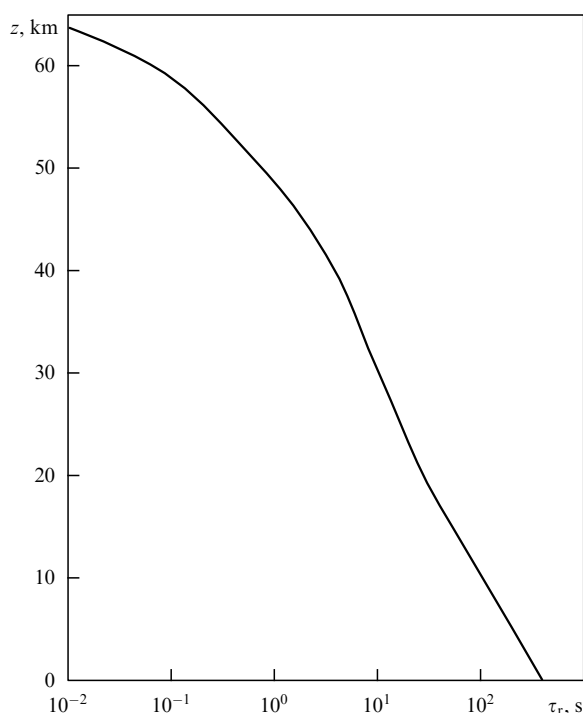


Figure 10. Dependence of the relaxation time τ_r on the altitude z .

It is natural to distinguish between two mechanisms of electric field generation. The first one is the usual smooth increase in the field inside and on the boundaries of the clouds under the action of atmospheric winds, gravitational force, and the trapping of charged particles by water droplets, ice particles, and aerosols. The characteristic time of this process is of the order of 1–10 min [35, 37, 38]. The second mechanism is a sharp change of the charge in a cloud as a result of a powerful electric discharge onto the Earth. The characteristic time of this process is in the millisecond range.

Comparing the characteristic times of these processes with the relaxation time leads us to the finding that a considerable excess of the field E over E_c (63) is possible only in the latter case. In a high-altitude region ($z \geq 20$ –50 km), as a result of the fast field relaxation, the RB conditions can be satisfied only over a rather short time $\Delta t \leq 10$ s. On the contrary, the first regular process can lead only to fields E close to or slightly exceeding E_c . But the lifetime of such a field may be as long as several minutes.

Fast field generation is obviously realized in upper layers of the thunderstorm atmosphere, where a strong RB can occur. The latter is possibly responsible for the giant high-altitude discharges that will be discussed at length in Section 6.

The process of regular field generation is significant in the main zone of thunderclouds at altitudes of 4–8 km, where RB proceeds softly as multiple micro-breakdowns. They have a strong effect on the electrodynamics of the thundercloud and are perhaps among the reasons for lightning generation. The role of these processes will be discussed in Section 7.

6. High-altitude atmospheric discharges

6.1 Optical observations of high-altitude discharges

Glowing discharges above thunderclouds have been observed for over a century [39–43]. However, optical instruments that

allowed reliably determining the characteristics and structure of these discharges, the frequency of their occurrence, and their optical brightness in various optical ranges were created only recently [44–56]. Measurements are carried out on spacecraft and on aeroplanes flying above thunderclouds; thunderstorms are also observed from the ground, near the horizon. High-sensitivity TV cameras are used for the observations.

An example of such high-altitude discharges from a thundercloud into the ionosphere is shown in Fig. 11. According to Refs [50–57], the discharge duration is 10–200 ms, the altitudes are 25–100 km, and the horizontal extent is 10–50 km. The glow-intensity peak is observed at an altitude of 50–60 km. The total volume of the radiating region normally exceeds 1000 km³ and the brightness is 10–100 kR [rayleigh is an off-system unit of measurement used in foreign literature; 1 R = 10⁶ photons (cm² s)^{−1}]. An extremely, (1–5) × 10³ kR bright burst of millisecond duration is seen against the average background [54]. The high-altitude discharge frequency above a large thunderstorm complex is small, about 0.01 s^{−1}. We note for comparison that, in analogous conditions, the frequency of negative discharges from clouds onto the Earth is of the order of 5 s^{−1} and that of positive discharges is 0.3 s^{−1} [35, 58, 59].

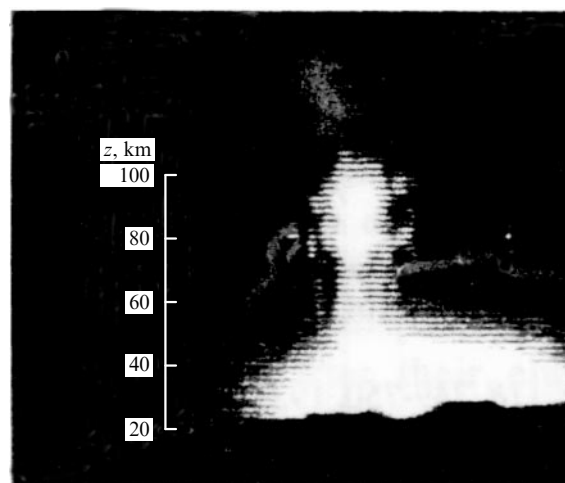


Figure 11. Example of a sprite discharge [52].

High-altitude discharges undoubtedly constitute a special class of electric discharges in the atmosphere, which differ appreciably from the ordinary lightning in their temporal and spatial characteristics.

6.2 Radio observations at very low frequencies

The effect of atmospheric discharges upon very-low-frequency (VLF) radio waves ($f \sim 10$ –30 kHz) propagating in the channel between the Earth's surface and the ionosphere have long been observed [60, 61]. They are commonly associated with the precipitation of electrons from the magnetosphere, due to the interaction with whistling atmospherics (whistlers). The characteristic time of the development of a perturbation in the lower atmosphere, caused by electron precipitation, is of the order of 5 s [61, 62].

Much more rapid processes that induce perturbations and are characterized by very short times of development (< 10 ms) have recently been discovered [61]. An example is

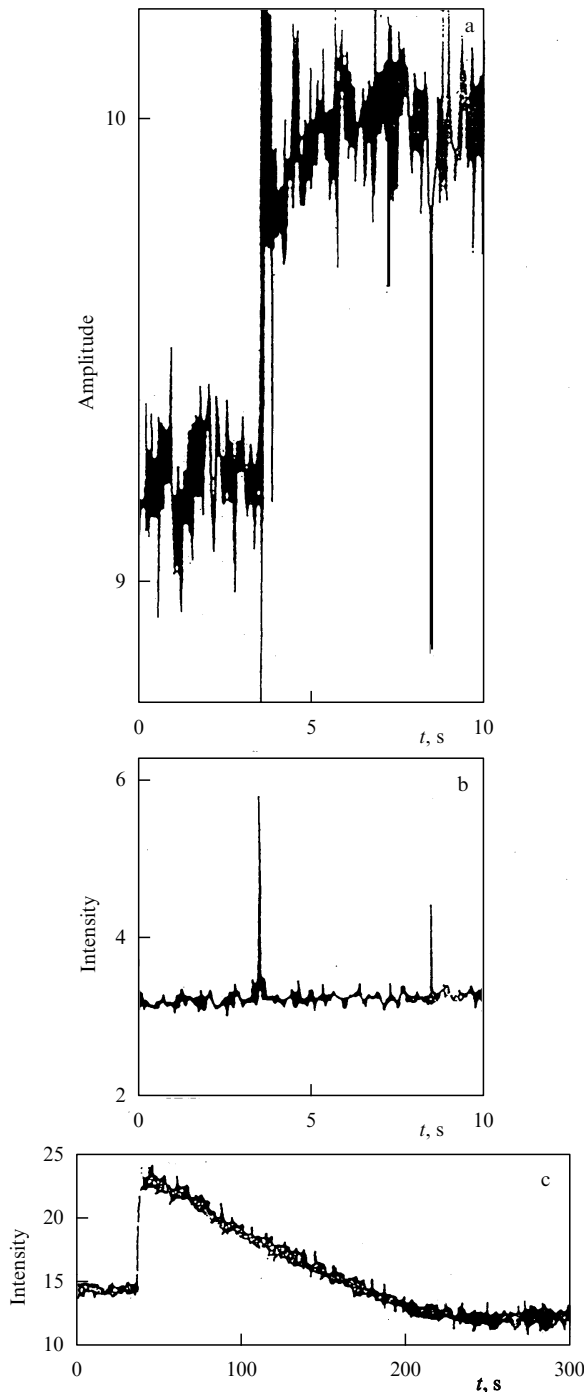


Figure 12. Jumps in (a) the VLF-signal amplitude and (b) in the intensity of radio atmospherics. (c) Relaxation of the intensity of the VLF-signal perturbation [61].

given in Fig. 12. At the moment of a VLF-signal jump at 28.5 kHz (Fig. 12a), the lightning discharge was recorded optically and by the occurrence of atmospherics (Fig. 12b). The development of a perturbation with a millisecond duration can only be due to the direct action of a lightning discharge on the lower ionosphere. However, an analysis of the relaxation of the VLF-signal perturbation (Fig. 12b) shows that the observed effect is due to precisely an increase in the plasma ionization in the lower ionosphere at altitudes of 60–85 km, because it is only an ionization perturbation that relaxes within a time of the order of tens of seconds.

Thus, the study of VLF radio-wave propagation demonstrates the presence of a substantial pulsed increase in the ionization in the lower ionosphere, apparently due to high-altitude discharges.

6.3 A model of high-altitude discharge

An important feature of the RB critical field is that it falls exponentially rapidly with altitude (63). At the same time, the air conductivity σ above 20–30 km is very high, so that, at altitudes of 20–50 km, the constant electric field vanishes owing to polarization within a time of the order of 10 s or even shorter. Therefore, in a quasi-stationary state the field is virtually absent there ($E \approx 0$).

However, after a strong positive discharge onto the Earth (a positive lightning carries a charge of up to 100 C or more [55, 35]), the balance is violated, and a field E that substantially exceeds the critical field can occur over a large space region for a short time (Fig. 13). The electric field is then directed to the Earth, i.e., it accelerates electrons towards the ionosphere. Over a broad discharge area ($S \geq 100 \text{ km}^2$), the flux of secondary cosmic ray seed electrons (64) is very large, and even within a time of the order of 1 ms their total number may be $10^6 - 10^7$.

A very simple model of such a system is shown in Fig. 13 [63]. In a cloud, 10 km in diameter, a layer of a positive 100-C charge is located at an altitude of 18 km, while the corresponding layer of negative charge lies at an altitude of 5 km. The electric field outside the cloud is screened by a polarization-induced negative charge located at an altitude of 25 km and by a positive charge at the lower boundary of the ionosphere, at an altitude of 70 km. Because of the screening, the field is virtually absent at altitudes $z > 25 \text{ km}$: $E = E_T + E_P \approx 0$.

As a result of a positive discharge Q , the field E_T disappears inside the cloud, and a considerable electric field E_P remains in the region between the upper boundary of the cloud and the ionosphere. The distribution of this field over z , along the axis of the system, 10 μs after the discharge is presented in Fig. 14. We can see that, over a large altitude

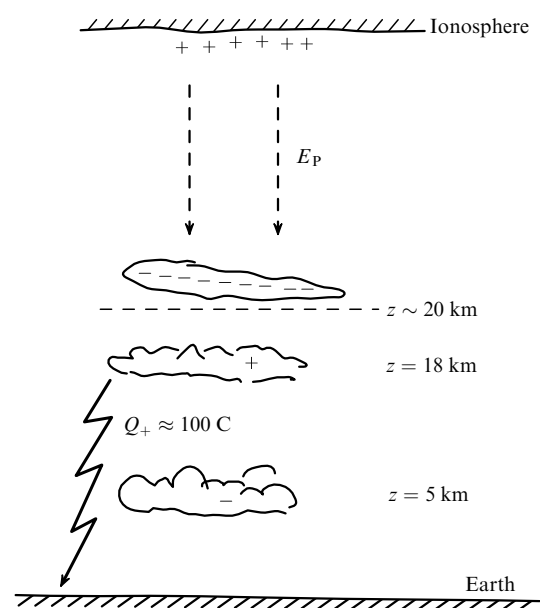


Figure 13. Model for the appearance of conditions for a high-altitude discharge.

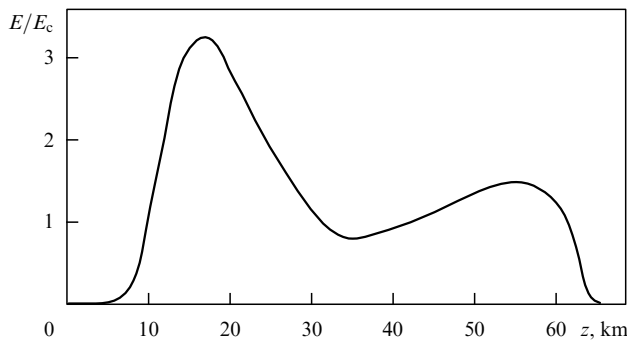


Figure 14. Dependence of the field E/E_c on the altitude z .

range (from 20 km up to the lower ionosphere), the field E exceeds the minimum runaway-breakdown field. For the appearance of a polarization field compensating E in the altitude range $z \leq 50$ km, a time of the order of several seconds is needed. In this period, it becomes possible for a giant high-altitude discharge to occur owing to a runaway breakdown. The number of characteristic ionization lengths ensuring the exponential RB growth is L/l_a . When an RB starts developing at an altitude of 20 km, this parameter is fairly high: $L/l_a \geq 20-40$. Owing to the exponential growth of the avalanche and the large number of seed electrons, the total number of high-energy electrons that create the discharge to altitudes of about 50 km may reach very high values of $10^{16}-10^{20}$. As a result of the diffusive beam broadening (see Section 4.5) the width of the RB discharge region at an altitude of 40–60 km reaches 30 km. We have given here only a simple example explaining the character of the principal processes. Numerical models allowing both for different initial charge distributions and for the development of the breakdown in time are considered in more detail in Refs [64–73]. The general picture of a high-altitude discharge remains unchanged, although details may, of course, differ noticeably.

As pointed out above, positive discharges inside clouds or from a cloud onto the Earth, which release negative charges of the order of or larger than 100 C, have repeatedly been observed during heavy thunderstorms [35, 58]. Moreover, positive discharges onto the Earth, accompanied by extremely large changes in the electric dipole moment, have systematically been observed (with a probability of 90%) simultaneously with high-altitude sprite discharges [55]. However, exceptions are also possible. For instance, according to Ref. [74], a sprite was observed after a strong negative discharge onto the Earth.

6.4 A model of optical emission

For high-energy electrons moving in air, the efficiency of the optical emission generated by them in different spectral regions is known [75–77]. In the conditions of interest, $\varepsilon \sim 0.1-10$ MeV, it is practically independent of the energy of fast electrons. This allows a rather accurate determination of the runaway-discharge emission at various altitudes, where blue radiation dominates below 50 km and red radiation at higher altitudes. It is such a pattern that is observed in sprite discharges. At ionospheric altitudes, in the upper part of a sprite discharge, red radiation dominates, and the discharge is smeared as the result of the diffusive beam scattering.

Let us note another important feature. The electric field E substantially exceeds the minimum field E_c in the vicinity of a

thundercloud (at altitudes of $z \sim 15-25$ km) and far from it (at altitudes of $z \sim 35-50$ km). This is easy to understand: at first, the decrease in the field E , determined by the increase in the distance from the charge, prevails and then the exponential fall of the atmospheric density, which strongly reduces E_c (3) starts dominating. Thus, two regions where a runaway breakdown can effectively develop, a near and a far one, can be distinguished. In the intermediate region ($z \sim 30-35$ km) it develops only at especially high values of the released charge Q . Qualitatively, this feature is always present and depends only slightly on the chosen model.

Detailed calculations of the high-altitude discharge in the RB model were carried out in a number of papers [63–73]. According to Refs [70, 73] the radiation due to a high-energy electron beam can create millisecond pulses of giant (several megarayleighs) intensity (Fig. 15). Much longer (several tens of milliseconds) generation of radiation with an intensity of tens of kilorayleighs is due to slower electrons. The results of the calculations agree with observational data [50–52, 56, 57].

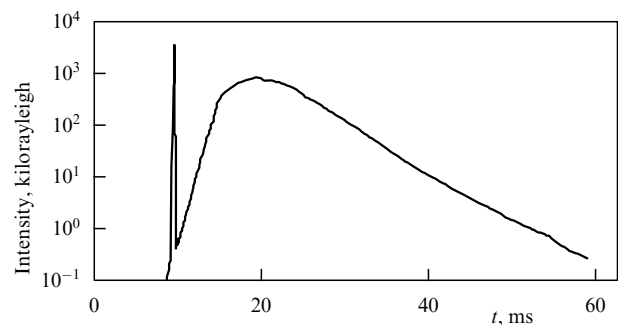


Figure 15. Time dependence of the radiation intensity [70].

It should be noted that this model proposed to explain the optical emission of a sprite discharge and based on RB only is not unique. Other possible mechanisms are also pointed out: breakdown in a radiation field created by a superpowerful intercloud discharge [78–80], breakdown in a quasi-static field [81–84], or a combination of these with an RB [63, 70]. Effects of meteors on sprite generation have also been reported [85, 86]. However, an important additional argument in favor of the direct relation between high-altitude discharges and RB are the observed intense gamma-ray pulses.

6.5 Gamma-ray bursts

The intense gamma-ray bursts observed on the *Compton* satellite [87, 88] can be regarded as a confirmation of the important role of RB in high-altitude discharges. It has been established that gamma bursts come from the regions of the most intense thunderstorm activity. The duration of gamma bursts is several milliseconds and their energy spectrum corresponds to the RB-produced spectrum. It can be noted that, compared to observations of X-ray emission in thunderclouds (see below), the spectrum is shifted toward high energies (with a maximum near 300–500 keV). This is indicative of a large electron acceleration length and substantial losses of gamma radiation in the atmosphere, which directly agrees with theory. The radiation intensity is very high [of order 100 photons $(\text{cm}^2 \text{ s})^{-1}$]. The results of model RB calculations are in reasonable agreement with observations of gamma-ray bursts [17, 63, 68, 89].

It should be emphasized that the one-to-one correspondence of high-altitude discharges and powerful gamma-emission pulses still remains a hypothesis although highly plausible. No data of direct and simultaneous observations of optical and gamma radiations from high-altitude discharges are yet available.

6.6 High-energy electrons in the magnetosphere

It was shown in Ref. [90] that, if the runaway-breakdown region reaches sufficiently high altitudes ($z \sim 65\text{--}75$ km), a considerable flux of electrons with energies of the order of or higher than 1 MeV can penetrate into the Earth's magnetosphere. Fast electrons scattered by waves in the magnetosphere will find themselves in a magnetic trap, and then, drifting in the magnetic field of the Earth, will gradually form a radiation belt. Thus, according to the hypothesis [90], high-altitude RB discharges can serve as a source of the inner radiation belt of the Earth.

6.7 Generation of electron–positron pairs

Intense bursts of gamma rays of energies reaching several mega-electron-volts should, according to the runaway breakdown theory, be accompanied by the production of electron–positron pairs [24].

According to Ref. [25], the generation of $N_{e^+e^-}$ pairs is related to gamma-ray emission as follows:

$$\frac{N_{e^+e^-}}{N_\gamma} = \frac{7}{9} \frac{N_\gamma}{N_e}.$$

Here, N_γ is the number of intense gamma quanta and N_e is the number of fast electrons. This relation makes it possible to estimate the magnitude of the expected effect of the generation of observed gamma-ray bursts:

$$N_{e^+e^-} \sim 10^6\text{--}10^{10},$$

where $N_{e^+e^-}$ is the total number of generated pairs. In observations they may show up as a narrow electron–positron annihilation line.

7. Lightning discharges in the atmosphere

We shall now discuss the effect of RB on a number of observed processes in the thunderstorm atmosphere within the region of regular electric-field generation ($z \sim 4\text{--}8$ km).

7.1 Maximum electric field

First of all, numerous observations show that the maximum electric fields E_{\max} in thunderclouds in the atmosphere are far from reaching the threshold fields for normal breakdown [58, 59, 35]. On the contrary, as will be seen below, they are close to the critical RB field E_c (63). Figure 16 gives examples of balloon measurements of the electric field in thunderclouds. The results are compared with the field $E_c(z)$ [91, 92]. We can clearly see an exponential fall of the maximum strength of the observed field E_{\max} with the altitude z , which perfectly agrees with formula (63). Another circumstance, no less important, is that at $E_{\max}(z) \approx E_c(z)$ lightning discharges (L) often occur, and the correlation is high. This fact has been specially stressed in recent publications (see, e.g., the most exhaustive contemporary monograph [35] devoted to thunderstorm electricity).

Thus, as was predicted for the first time in Ref. [1], the critical runaway-breakdown field and its altitude dependence

have a decisive effect on the actual distribution of thunderstorm fields in the atmosphere. This suggests that the principal electrodynamic processes during a thunderstorm and perhaps also the generation of lightning discharges are intimately related to RB. Below we present other confirmations for the substantial RB effect upon thunderstorm processes.

7.2 Anomalous X-ray bursts

Strong and fairly long X-ray bursts have been discovered in the energy range of 30–120 keV. In airborne [93] and balloon [94–96] observations, the intensity of X-ray emission increased within several seconds by two or three orders of magnitude compared to the standard background due to cosmic rays. An example is given in Fig. 17. Measurements were performed on a balloon rising in a thundercloud at a velocity of 5 m s^{-1} . We can see that the total duration of the X-ray burst was longer than 1 min. Its development and the intensity falls correlate with the occurrence of lightnings. Analogous X-ray bursts have recently been discovered in high-altitude (12 km) balloon observations near the upper boundary of thunderclouds (the so-called ‘anvil’) [97].

According to the theory [1], X-ray bursts are associated with multiple runaway micro-breakdowns (RMB) that occur over vast areas of the order of several square kilometers. Since thunderclouds have a plane-layered structure, the mean electric field in them is close in direction to the vertical z ; then, if the conditions (61) and (63) hold, each secondary electron of cosmic rays generates a runaway avalanche in the thundercloud. The number of fast electrons will thus grow rapidly. This process, called RMB, is precisely the reason for the observed X-ray bursts.

The calculation results [98] for the intensity and spectrum of RMB-induced X-ray radiation are plotted in Fig. 18, which shows that the spectrum is surprisingly stable and depends only slightly on the position of the observer. It always has a pronounced peak in the region of 50–60 keV and falls rapidly towards both low energies (owing to photoionization) and high energies, 100–150 keV (owing to Compton losses). As to the X-ray radiation intensity, it reaches its maximum in the vicinity of the electric field maximum, i.e., the X-ray radiation maximum is shifted by about 100–200 m in the direction of electron motion (see Fig. 18). It is very important that, away from the maximum, the X-ray radiation intensity falls sharply (see Fig. 18), and even at a distance of the order of 1–1.5 km from the electric-field maximum it is virtually undistinguishable from the background.

The above-presented calculation results for anomalous X-ray bursts due to RMB suggest two conclusions important for observations:

- (1) the spectrum has a standard form with a characteristic maximum in the region of 50–60 keV;
- (2) intense radiation can be observed only within 1–1.5 km altitude limits from the electric-field maximum. This means that X-ray emission from RMB can actually be observed only for $z \geq 2.5\text{--}3$ km since, according to numerous measurements, values $|E| \sim E_c$ are reached in thunderclouds only at altitudes $z \geq 4$ km (see Fig. 16).

Both conclusions are confirmed by observations [93–97]. It should also be noted that, according to calculations [98], appreciable increases in the number of fast electrons and in the X-ray emission generated by these electrons occur already in pre-breakdown conditions, as the field E approaches E_c (more precisely, for $E > 0.95E_c$).

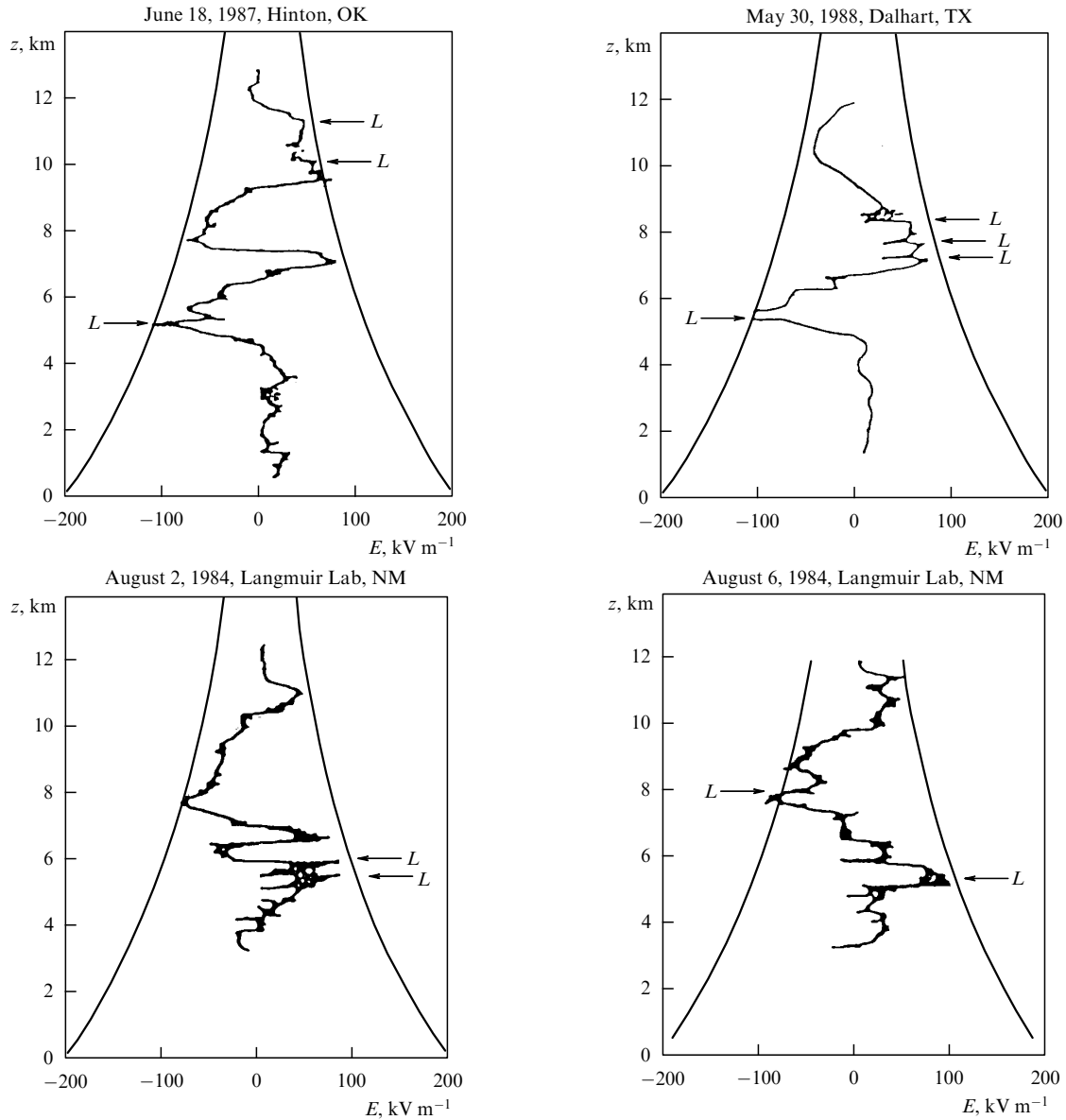


Figure 16. Comparison of the altitude (z) dependence of the balloon-measured electric field E with that of the critical field $E_c(z)$. The arrows L mark lightning events [91].

7.3 Anomalous growth of conductivity

The conductivity σ of the atmosphere is determined by the ionization of air by cosmic rays. In the presence of clouds or rainfall near the Earth's surface (at altitudes of up to 2 km), a significant contribution is made by the radiation of radioactive elements. In a clear sky, the ion concentration is of the order of 10^3 cm^{-3} , which corresponds to an electric-field relaxation time of $\tau_r = (4\pi\sigma)^{-1} \approx 400 \text{ s}$ (see Fig. 10). The conductivity $\sigma \propto \nu_m^{-1}$ increases rapidly with altitude owing to the decrease in the number of collisions ν_m as the molecule concentration N_m falls (see Fig. 10). In clouds, on the contrary, the conductivity may lower owing to the attachment of charges to water droplets and aerosols [35].

As an RMB occurs, the number of high-energy electrons and, accordingly, the number of ionization events in a layer 100–500 m thick strongly increase in the vicinity of the thunderstorm-field maximum (see Fig. 9). Correspondingly, the X-ray radiation intensity also grows sharply (see Fig. 18). Using the experimental data [94, 95] on the increase of

the X-ray radiation intensity ($10^2 - 10^3$) we can estimate the number of exponents in the accelerating layer $z \sim (5-6)l_a$ under the actual conditions and thus determine the number of fast electrons generated by one primary particle. It is, however, of importance that, according to the RB theory, the distribution function of fast electrons increases effectively with decreasing electron energy not only for $\varepsilon > \varepsilon_c$ (4), but also in the region of low energies $\varepsilon < \varepsilon_c$ (41) (see Figs 4, 8). All these electrons — both high-energy ($\varepsilon > \varepsilon_c \sim 10^2 \text{ keV}$) and fairly low-energy (up to the maximum ionization cross section, $\varepsilon \sim 0.1-1 \text{ keV}$) ones — make a substantial contribution to the ionization of the atmosphere. For this reason, the free-electron generation intensity Q_e in a layer of thickness of order l_a increases appreciably near the RB-region boundary:

$$Q_e = \frac{dN_e}{dt} = \int f(\varepsilon) d\varepsilon \approx Q_0 \exp\left(\frac{L}{l_a}\right) \ln^2 \frac{\varepsilon_c}{\varepsilon_i}. \quad (66)$$

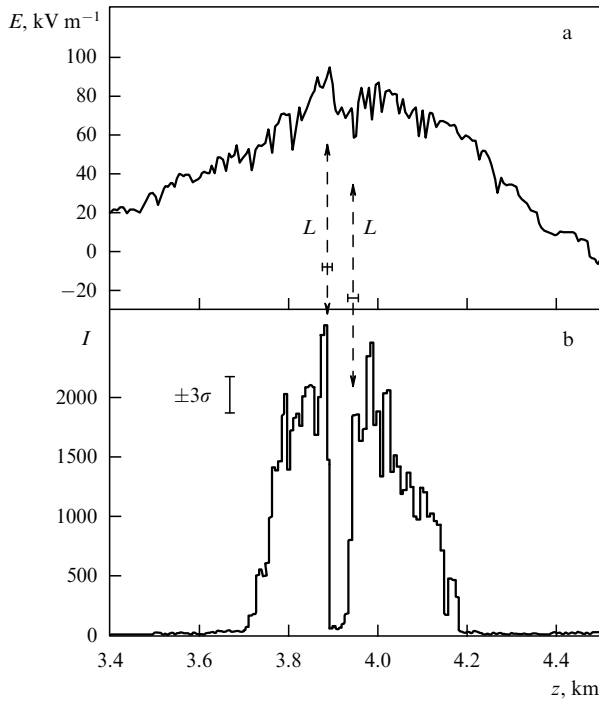


Figure 17. (a) Electric field E and (b) intensity I of X-ray radiation as functions of altitude z during a burst for $3.7 \leq z \leq 4.2$ km. At altitudes $z < 3.7$ km and $z > 4.2$ km the background of X-ray radiation is standard [94].

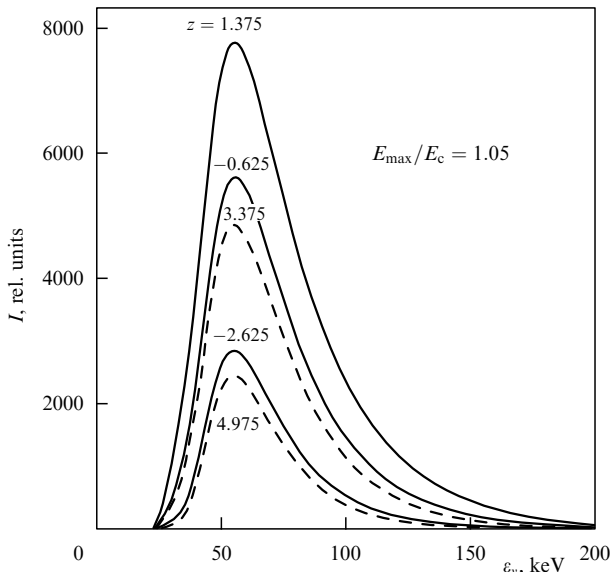


Figure 18. Dependence of the X-ray radiation intensity on the energy of quanta ε_v for various z values. The altitude z is expressed in the units of l_a (9) (in clouds, $l_a \sim 70$ – 100 m) and is measured from the position of the electric-field maximum E_{\max} (58). The value of E_{\max}/E_c is indicated in the figure.

Here, Q_0 is the intensity of free-electron generation by the cosmic-ray flux in the atmosphere; L is the size of the RB region, i.e., the region where $E(z) \geq E_c$; and ε_i is the mean air-molecule ionization energy. The integration in (66) takes into account the expressions for the distribution function (41), (56).

It is noteworthy that all newly born electrons that initially have an energy of several electron-volts lose it within a very

short time of $\sim 10^{-8}$ s owing to inelastic interactions with air molecules [31]. Furthermore, because of triple collisions, electrons attach themselves rapidly to O_2 and H_2O molecules to form negative ions [31]. The characteristic lifetime of a free electron at altitudes of thunderclouds is as short as about 70–100 ns [99, 100]. Thus, electrons disappear rather rapidly, but at the same time, the densities of positive (N_i^+) and negative (N_i^-) ions in the perturbed layer of the atmosphere increase. It is the ions that determine the increase of the conductivity in the RMB region (although, as noticed in Ref. [100], the electrons can contribute to the increase of conductivity, in spite of their very short lifetime).

Let us estimate the contribution due to ions. The growth of ion concentration N_i^\pm in air is

$$\frac{dN_i}{dt} = -\alpha_{ri} N_i^2 + Q_i. \quad (67)$$

Here, Q_i is the ion source and α_{ri} is the recombination coefficient of ions ($\text{cm}^3 \text{s}^{-1}$) determined by triple collisions [31]:

$$\alpha_{ri} \simeq 8 \times 10^{-6} \frac{N_m}{2.7 \times 10^{19}} \left(\frac{300}{T} \right)^{5/2}. \quad (68)$$

Under normal conditions, i.e., in the absence of a runaway breakdown, the total ionization by cosmic rays yields $Q_0 = 3 \text{ cm}^{-3} \text{s}^{-1}$. Then, for stationary conditions, we obtain from (67) and (68):

$$N_i \approx 10^3 \text{ cm}^{-3}, \quad \sigma_i \approx 2 \times 10^{-4} \text{ s}^{-1}, \quad \tau \approx 400 \text{ s}.$$

These estimates are typical of fine weather and their values and altitude dependence are well studied [32–36].

The situation changes radically under RMB conditions. The ion source $Q_i = Q_e$ is described by formula (66); therefore, we find

$$N_i \approx (5-8) \times 10^4 \text{ cm}^{-3}, \quad \sigma_i \approx (2-3) \times 10^{-2} \text{ s}^{-1}, \quad \tau \approx (4-6) \text{ s}.$$

Thus, under RMB conditions in a thundercloud, within a time of several tens of seconds, the ion concentration increases by 1.5–2 orders of magnitude [100]. A layer of anomalously high conductivity appears, which should naturally have a strong effect on the electrodynamic processes in the thundercloud.

We emphasize that, according to calculations [98], the number of fast electrons changes many-fold as the ratio E/E_c changes by a mere 10% (see Fig. 9, $0.9 \leq E/E_c \leq 1.1$). For this reason, in the real conditions of a thundercloud, the ion concentration and, therefore, the anomalously high conductivity occurring in the layer at $E \approx E_c$ can also change radically. Thus, the above estimates only refer to the ‘average anomalous conductivity’. The actual conductivity may, however, exhibit strong fluctuations, including spatial fluctuations inside the layer, and the departures of the conductivity from this average may severalfold exceed the latter.

Note that the above-presented estimate of the increase in the conductivity should be treated as a preliminary one. It disregarded, for instance, the absorption of free ions by water droplets, ice particles, and aerosols in the thundercloud, and inverse processes. The role of collisions between fast electrons and the same particles and the whole sequence of changes

related to the complex physico-chemical processes in clouds were also neglected. However, all these processes may turn out to be slower than RMB.

The phenomenon of anomalous growth in conductivity for $E > E_c$ was predicted in Ref. [1] (where it was called 'fast charge transfer'). Its experimental realization was indirectly confirmed in Refs [99, 100] by analysis of observational data [94, 95].

7.4 Radio-interferometric measurements

Let us briefly discuss some results of radio-interferometric measurements carried out at a frequency of 27 MHz during a period of thunderstorm activity [99]. The interferometer consisted of five antennas and made it possible to localize the radiation source on the celestial hemisphere to an accuracy of the order of 1° , i.e., approximately within a thundercloud region 20–100 m in size. The high temporal resolution of the system (no worse than 1 ms) allowed a thorough investigation of not only the development of a lightning discharge itself, but also the foregoing processes. The data of Ref. [101] indicate that during the 100–500 ms prior to the appearance of the first pulse of a lightning discharge, activity is observed over an extensive (one or several kilometers large) cloud region. This process can be represented as slowly drifting, multiple, small-scale discharge currents. Each burst of radiation was localized inside the interferometer resolution region (50 m), but the centers of the emitting regions moved continuously. The activity increased to a strong radiation burst. In this period, the radiation intensity first went on increasing rapidly and then fell sharply within a time shorter than 1 ms. Simultaneously, the electric field decreased abruptly, apparently as the result of the first lightning stroke. Such processes with characteristic time of development of the order of 0.1–1 s precede the main discharge, which typically consists of several lightning strokes both inside the clouds and onto the Earth.

7.5 Generation of a lightning

A lightning discharge due to the creation of a highly conductive channel and the accumulation of the electric charge of a thundercloud from an area of 1–100 km² within a time of 1–10 s is a very complicated process, which has been investigated in numerous studies (see, e.g., monographs [58, 59, 35, 102]). We will note here only a few new points associated with the role of runaway breakdown.

This is, first, the above-mentioned RMB-induced anomalous increase in conductivity. The increase in conductivity should naturally promote the fast transfer of the electron charge distributed in the cloud. Although large, the indicated increase in conductivity seems to be insufficient, 'on average', for gathering the electric charge. It may, however, grow substantially owing to the above-mentioned strongly nonuniform, random structure of the conductive zone. The latter can promote the formation of effective conductive channels. It is possible that precisely this, RMB-conditioned 'fractal' behavior of conductivity in a cloud layer prior to the first lightning discharge is partially reflected by the radio-interferometric observations [101] described in the previous section. Note that the possibility of the appearance of a fractal structure conductivity in a cloud, caused by small-scale normal discharges, is discussed in papers [103, 38, 104, 105].

The rapid, RMB-induced variation of the ion concentration should lead not only to an increase in conductivity but

also to the violation of the quasi-stationary dynamic balance determined by the action of gravitational and electric fields, as well as the action of wind upon various components of charged particles (ions, droplets, ice particles, aerosols) in the thundercloud. The violation of the dynamic balance results in rapid nonstationary processes, which may also favor the appearance of electric discharges. The possibility of generation of a 'step leader' under RMB conditions, which occurs at the initial stage of lightning development, was pointed out in Ref. [1]. A more detailed calculation of this process is presented in Refs [106, 124].

Finally, the break of the quasi-stationary state that induces lightning generation can be caused by the joint action of RB and a high-energy ($\varepsilon \geq 10^{15} - 10^{16}$ eV) cosmic particle generating an extensive air shower (EAS) with $10^6 - 10^7$ secondary electrons. According to theory [107], this process can instantly (within microseconds) form a local, strongly elongated and highly ionized region where conditions for the origin of a streamer are present, which can serve as a lightning seed. The appearance of high-energy radiation at the initial stage of lightning discharge was noted in Refs [122, 123].

On the whole, we can suppose that the correlation between lightnings and runaway breakdown revealed from measurements of electric fields (see Fig. 16) and observations of X-ray bursts (see Fig. 17) is physically grounded and reflects the real effect of RB and RB-induced processes upon lightning generation. However, the investigation of this problem is currently at a very early stage.

8. Cosmic rays and electrodynamic processes in the Earth's atmosphere

The possibility of the mutual influence of cosmic rays and electrodynamic processes in the atmosphere was first noted by Wilson [14]. This is, first, an additional increase in the energy of cosmic particles affected by electric fields in thunderclouds. The effect predicted by Wilson has repeatedly been studied and, to a certain extent, confirmed in experiment [108–118]. Second, it is cosmic particles that determine ionization and, therefore, conductivity and electric currents in the Earth's atmosphere. These phenomena, including the altitude and latitude dependences of the atmospheric ionization due to cosmic rays, have not only been confirmed by experiment, but also analyzed at length [32–36].

The situation changed radically after runaway breakdown was discovered. The relation between cosmic rays and electric phenomena proved to be much deeper. It became clear that cosmic rays significantly affect the state of thunderclouds and apparently have a strong effect on both ordinary lightning discharges and the new types of giant atmospheric discharges between clouds and the ionosphere (sprites). It is possible that the main role is played here not only by the bulk of cosmic particles, but also by individual high-energy particles ($\varepsilon \sim 10^{14} - 10^{16}$ eV), which generate extensive air showers of cosmic rays. At the same time, the inverse effect of the influence of thunderstorm electric fields on cosmic rays is observed, which shows up in a strong local increase of the number of electrons of not very high energies ($\varepsilon \leq 10^6$ eV) and in a sharp intensification of X-ray and gamma emission.

The conclusion that there is a more intimate relation between electric processes in thunderstorm atmosphere and

cosmic rays suggests itself. This means that complex studies of both groups of phenomena are necessary. Such works have already been started at the FIAN (P N Lebedev Physics Institute) cosmic-ray station located in the mountains of Tien-Shan at an altitude of 3340 m [119]. In addition to the unique instrumentation for studying extensive air showers, the station is equipped with a system of counters, antennas, and sound detectors to record X-ray emission from RB and lightnings. The first investigation carried out during a thunderstorm period in the fall of 1999 singled out X-ray bursts, 2–5 min long, that marked RBs (Fig. 19) [120]. These bursts are quite analogous in their principal characteristics — energies of quanta and photon-flux intensities — to those observed earlier on balloons [94–96]. Over all points of observation, separated by about 500 m, these bursts are well correlated, and hence the observed X-ray radiation is emitted simultaneously over an extensive spatial region, which is also typical of an RB in a thundercloud. Further studies will include simultaneous observations of EAS and X-ray emission from RBs, neutron radiation near the Earth's surface, and radio-frequency and acoustic radiation from lightnings. Note also that the Baksan neutrino laboratory has renewed studies of the effects of thunderstorms on cosmic rays [109]. In addition, it is planned to carry out systematic measurements of the electric field near the Earth's surface, which will make it possible to accurately record lightning discharges, and to widely develop radio observations, including radio interferometry at various frequencies and radiometric studies of the lower ionosphere. Also, tied balloons will possibly be used to perform direct measurements in thunderclouds. A whole complex of measuring equipment localized at one place will help to simultaneously obtain various data on the processes in thunderclouds and thus give a deeper insight into their physical nature.

Let us point out an important advantage of high-altitude stations. As mentioned above, effective observations of the

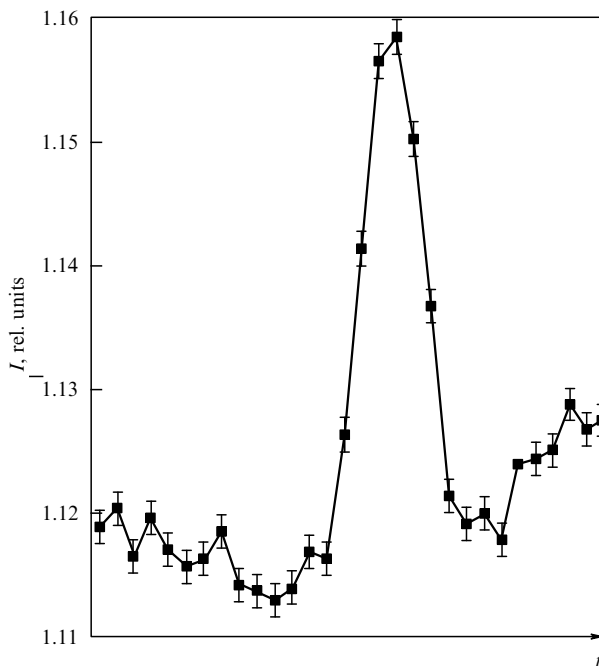


Figure 19. X-ray radiation intensity during an RB; each point corresponds to data averaged over 1 min.

X-ray radiation from RBs are possible only at sufficiently high altitudes ($z \geq 3$ km). The reason is that thunderclouds and the related strong electric fields are mostly situated at altitudes of $z \sim 4$ –8 km, and X-ray quanta can propagate in the atmosphere at these altitudes only over distances of the order of 1 km or less.

9. Laboratory experiment

Laboratory investigations of RBs are undoubtedly of interest. However, it is extremely difficult to perform such an experiment. As concerns gas breakdown, the main difficulty is the scale condition (61). For instance, in air at a pressure of $p \sim 1$ atm, the length is $l_a \sim 50$ m.

Cyclotron resonance and magnetic trapping were used [121] to overcome this difficulty. The acceleration of an electron under the action of an alternating electric field $E = E_0 \cos \omega t$ in the conditions of cyclotron resonance,

$$\omega = \omega_B = \frac{eB}{mc}, \quad (69)$$

is quite similar to the acceleration by a constant field. However, a noticeable difference exists. First, owing to the relativistic effect, the electron mass increases with the increase energy ($m \sim \varepsilon \sim \gamma - 1$) of this electron, which entails resonance detuning (69). Second, to trap electrons, it is necessary to use a magnetic trap with a magnetic field increasing towards the edge (a magnetic mirror), which also violates the resonance condition (69).

A relevant experiment was realized in Ref. [121]. In a trap with a magnetic field of $B \sim 1$ –3 kG, an alternating electric field with a frequency of 2.45 GHz was created. As soon as a certain electric-field amplitude is attained in an experiment, an avalanche-like growth in the number of accelerated electrons sets in and intense X-ray emission is observed (within a range of 100–300 keV) (Fig. 20). The emission is accompanied by a rapid electromagnetic-wave-energy absorption and, after a certain delay, by the excitation of the second cyclotron harmonic and strong optical radiation (see Fig. 20). Consequently, the energy of the field is first absorbed by fast electrons and then transferred to slow electrons. Thus, in spite of the noted features of cyclotron resonance, the principal RB mechanism associated with electron acceleration and the occurrence of a runaway particle flux remains unchanged.

The laboratory studies confirmed that runaway breakdown is in principle possible.

It is also possible in dense matter, where the runaway-electron avalanche length is $l_a \sim 0.1$ –10 cm. The detector size is therefore insignificant here. The main problem is the creation of sufficiently strong electric fields.

10. Conclusion

To summarize, we conclude that runaway breakdown, the new physical phenomenon predicted in 1992, has now been thoroughly studied theoretically and used extensively to interpret the important phenomena observed in the thunderstorm atmosphere. It apparently controls giant high-altitude discharges, anomalous X-ray bursts, powerful gamma-ray bursts, etc. One of the main factors determining the possibility of runaway breakdown in the atmosphere are cosmic rays. That is why the above-mentioned new effects

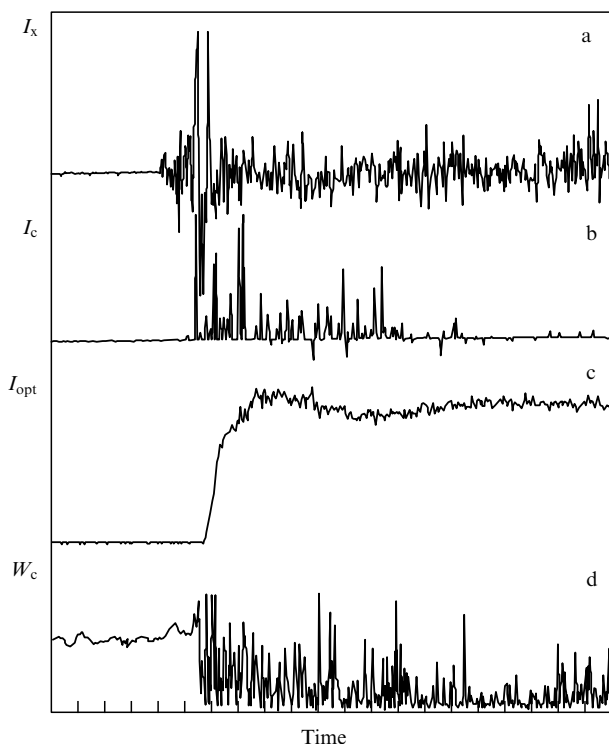


Figure 20. Cyclotron runaway breakdown in a magnetic trap. Time dependences (one division corresponds to 20 ms) are shown for (a) the intensity of X-ray radiation with energies $\varepsilon_v > 100$ keV (negative pulses occur when the flux of quanta exceeds the spectrometer temporal resolution), (b) the intensity of the second cyclotron harmonic, (c) the optical-radiation intensity, and (d) the cyclotron-wave ($f = 2.45$ MHz) power after the passage through the chamber.

reflect a deep relation between cosmic rays and thunderstorm processes in the atmosphere.

At the same time, it should be noted that the laboratory studies of runaway breakdown have only made their first steps. The realization and employment of this phenomenon in both gaseous and, in particular, dense media may open very interesting prospects. It should be hoped that necessary attempts in this direction will be made.

The authors express their gratitude to V L Ginzburg for his attention to this work, to R Roussel-Dupre for numerous helpful discussions, and to G M Milikh, K F Sergeichev, and A P Chubenko for fruitful collaboration. This work was supported by Russian Foundation for Basic Research (grant 00-15-96594) and EOARD–ISTC (grant 2236p).

References

- Gurevich A V, Milikh G A, Roussel-Dupre R *Phys. Lett. A* **165** 463 (1992)
- Mesyats G A, Korolev Yu D *Fizika Impul'snogo Probnya Gazov* (Physics of Pulsed Breakdown in Gases) (Moscow: Nauka, 1991)
- Raizer Yu P *Fizika Gazovogo Razryada* (Physics of Gas Discharge) (Moscow: Nauka, 1992) [Translated into English (Berlin: Springer, 1997)]
- von Engel A, Steenbeck M *Elektrische Gasentladungen, Ihre Physik und Technik* Vols 1, 2 (Berlin: Springer, 1932, 1934) [Translated into Russian (Moscow–Leningrad: ONTI, 1935)]
- Loeb L B *Fundamental Processes of Electrical Discharges in Gases* (New York: J. Wiley & Sons, 1939) [Translated into Russian (Moscow: Gostekhizdat, 1950)]
- Granovskii V L *Elektricheskii Tok v Gazakh* (Electric Current in Gases) (Moscow–Leningrad: GITTL, 1952)
- Meek J M, Craggs J D (Eds) *Electrical Breakdown of Gases* (Chichester: Wiley, 1978) [Translated into Russian (Moscow: IL, 1980)]
- Harvey A F *Microwave Engineering* (London: Acad. Press, 1963)
- Bethe H A *Ann. Phys. (Leipzig)* **5** 325 (1930)
- Gurevich A V *Zh. Eksp. Teor. Fiz.* **39** 1296 (1960) [*Sov. Phys. JETP* **12** 904 (1961)]
- Parail V V, Pogutse O P, in *Voprosy Teorii Plazmy* Issue 11 (Reviews of Plasma Physics) (Moscow: Energoizdat, 1982) p. 5
- Knoepfel S, Spong E *Nucl. Fusion* **19** 785 (1979)
- Landau L D, Lifshitz E M *Elektrodinamika Sploshnykh Sred* (Electrodynamics of Continuous Media) (Moscow: Nauka, 1970) [Translated into English (Oxford: Pergamon Press, 1984)]
- Wilson C T R *Proc. R. Soc. London* **37** 32D (1925)
- Babich L P, Loiko T V, Tsukerman V A *Usp. Fiz. Nauk* **160** 49 (1990) [*Sov. Phys. Usp.* **33** 27 (1990)]
- Gurevich A V, Milikh G M, Roussel-Dupre R A *Phys. Lett. A* **187** 197 (1994)
- Roussel-Dupre R A et al. *Phys. Rev. E* **49** 2257 (1994)
- Lehtinen N G et al. *Geophys. Res. Lett.* **24** 2639 (1997)
- Babich L P, Kutsik I M *Teplofiz. Vys. Temp.* **33** 191 (1995)
- Symbalisty E et al. *EOS Trans. AGU* **78** 4760 (1997)
- Babich L P et al. *Phys. Lett. A* **245** 460 (1998)
- Gurevich A V et al. *Radio Sci.* **31** 1541 (1996)
- Gurevich A V, Zybin K P *Phys. Lett. A* **237** 240 (1998); **243** 362 (1998)
- Gurevich A V et al. *Phys. Lett. A* **275** 101 (2000)
- Berestetskii V B, Lifshitz E M, Pitaevskii L P *Relyativistskaya Kvantovaya Teoriya* Vol. 1 (Relativistic Quantum Theory) (Moscow: Nauka, 1968) [Translated into English (Oxford: Pergamon Press, 1971)]
- Landau L D *Zh. Eksp. Teor. Fiz.* **7** 203 (1937)
- Lifshitz E M, Pitaevskii L P *Fizicheskaya Kinetika* (Physical Kinetics) (Moscow: Nauka, 1979) [Translated into English (Oxford: Pergamon Press, 1981)]
- Landau L D, Lifshitz E M *Kvantovaya Mekhanika* (Quantum Mechanics) (Moscow: Nauka, 1948) [Translated into English (Oxford: Pergamon Press, 1977)]
- Bethe H A, Ashkin J, in *Experimental Nuclear Physics* Vol. 1 (Ed. E Segre) (New York: Wiley, 1953) p. 277
- MacDonald A D *Microwave Breakdown in Gases* (New York: Wiley, 1966) [Translated into Russian (Moscow: IL, 1969)]
- Gurevich A V, Borisov N D, Milikh G M *Physics of Microwave Discharges* (Amsterdam: Gordon and Breach, 1997)
- Bazilevskaya G A, Svirzhevskaya A K *Space Sci. Rev.* **85** 431 (1988)
- Fulks J, Meyer P J *Geophys.* **40** 751 (1974)
- Daniel R R, Stephens S A *Rev. Geophys. Space Sci.* **12** 223 (1974)
- MacGorman D R, Rust W D *The Electrical Nature of Storms* (New York: Oxford Univ. Press, 1998)
- Ermakov V I et al. *J. Geophys. Res.* **102** 23413 (1997)
- Trakhtengerts V Yu, Mareev E A, Sorokin A E *Izv. Vyssh. Uchebn. Zaved. Radiofiz.* **40** 123 (1997)
- Iudin D N, Trakhtengerts V Yu, Preprint IPF RAN No. 482 (Moscow: IPF RAN 1998)
- Everett J D, Everett W H *Nature* **68** 599 (1903)
- Boys C V *Nature* **118** 749 (1926)
- Malan D C R *Acad. Sci.* **205** 812 (1937)
- Wilson C T R *Proc. R. Soc. London* **236** 297 (1956)
- Gales D M *Weatherwise* **35** 72 (1982)
- Vaughan O H, Vonnegut B J *Geophys. Res.* **94** 13179 (1989)
- Fisher J R *Weather* **45** 451 (1990)
- Franz R C, Nemzek R J, Winckler J R *Science* **249** 48 (1990)
- Boeck W L, Vaughan O H, Blakeslee R *EOS. Trans. AGU* **72** 171 (1990)
- Winckler J R, Franz R C, Nemzek R J *J. Geophys. Res.* **98** 8775 (1993)
- Vaughan O H (Jr.) et al. *Month. Weather Rev.* **120** 1459 (1992)
- Lyons W A *Geophys. Res. Lett.* **21** 875 (1994)
- Sentman D D, Wescott E M *Geophys. Res. Lett.* **20** 2857 (1993)
- Sentman D D et al. *Geophys. Res. Lett.* **22** 1205 (1995); Wescott E M et al. *Geophys. Res. Lett.* **22** 1209 (1995)
- Boeck W L et al. *J. Geophys. Res.* **100** (D1) 1465 (1995)

54. Winckler J R et al. *J. Geophys. Res.* **101** 6997 (1996)
55. Boccippio D J et al. *Science* **269** 1088 (1995)
56. Wescott E M et al., Preprint (University of Alaska, 1997)
57. Rairden R L, Mende S B *Geophys. Res. Lett.* **22** 3465 (1995)
58. Uman M A *The Lightning Discharge* (Orlando: Acad. Press, 1987)
59. Imenitov I N, Chubarina E B, Shvarts Ya M *Elektrichestvo Oblakov* (Cloud Electricity) (Leningrad: Gidrometeoizdat, 1971)
60. Inan U S, Knifsend F A, Oh J J *J. Geophys. Res.* **95** 17217 (1990)
61. Inan U S, AGARD Report (1995)
62. Sampath H T, Inan U S, Johnson M P *J. Geophys. Res.* **105** 183 (2000)
63. Roussel-Dupre R, Gurevich A V *J. Geophys. Res.* **101** 2297 (1996)
64. Pasko V P, Inan U S, Bell T F *Geophys. Res. Lett.* **23** 649 (1996)
65. Taranenko Y, Roussel-Dupre R *Geophys. Res. Lett.* **23** 571 (1996)
66. Bell T F, Pasko V P, Inan U S *Geophys. Res. Lett.* **22** 2127 (1995)
67. Symbalisty E M D, Roussel-Dupré R A, Yukhimuk V A *IEEE Trans. Plasma Sci.* **26** 1575 (1998)
68. Roussel-Dupre R et al. *J. Atmos. Sol. Terr. Phys.* **60** 917 (1998)
69. Yukhimuk V et al. *J. Geophys. Res.* **103** 11473 (1998)
70. Yukhimuk V, Roussel-Dupré R, Symbalisty E M D *Geophys. Res. Lett.* **26** 679 (1999)
71. Pasko V P, Inan U S, Bell T F *Geophys. Res. Lett.* **25** 2123 (1998)
72. Lehtinen V, Bell T, Inan U S *J. Geophys. Res.* **104** 24699 (1999)
73. Yukhimuk V et al. *Geophys. Res. Lett.* **25** 3289 (1998)
74. Barrington-Leigh C et al. *Geophys. Res. Lett.* **26** 3605 (1999)
75. Davidson G, O'Neil R J. *Chem. Phys.* **41** 3946 (1964)
76. Hartman K B *Planet. Space Sci.* **16** 1315 (1968)
77. Mitchell K B *J. Chem. Phys.* **53** 1795 (1970)
78. Milikh G M, Papadopoulos K, Chang C L *Geophys. Res. Lett.* **22** 85 (1995)
79. Valdivia J A, Milikh G, Papadopoulos K *Geophys. Res. Lett.* **24** 3169 (1997)
80. Nunn D, Rodger C *Geophys. Res. Lett.* **26** 3293 (1999)
81. Pasko V P, Inan U S, Bell T F *Geophys. Res. Lett.* **23** 649 (1996)
82. Pasko V P, Inan U S, Bell T F *Geophys. Res. Lett.* **23** 301 (1996)
83. Sukhorukov A I, Rudenchik E A, Stubbe P *Geophys. Res. Lett.* **23** 2911 (1996)
84. Veronis G, Pasko V, Inan U *J. Geophys. Res.* **104** 12645 (1999)
85. Suszcynsky D M et al. *J. Geophys. Res.* **104** 31361 (1999)
86. Symbalisty E M D et al. *Icarus* **148** 65 (2000)
87. Fishman G J et al. *Science* **264** 1313 (1994)
88. Nemiroff R J, Bonnell J T, Norris J P *J. Geophys. Res.* **102** 9659 (1997)
89. Lehtinen N G et al. *Geophys. Res. Lett.* **23** 2645 (1996)
90. Lehtinen N G et al. *Geophys. Res. Lett.* **27** 1095 (2000)
91. Marshall T, McCarthy M, Rust W *J. Geophys. Res.* **100** 7097 (1996)
92. Marshall T, Rust W, Stolzenberg H J *Geophys. Res.* **100** 1001 (1996)
93. McCarthy M, Parks G *Geophys. Res. Lett.* **12** 393 (1985)
94. Eack K B et al. *J. Geophys. Res.* **101** 29637 (1996)
95. Eack K B *Rev. Sci. Instrum.* **67** 2005 (1996)
96. Eack K B et al. *Geophys. Res. Lett.* **23** 2915 (1996)
97. Eack K B et al. *Geophys. Res. Lett.* **27** 185 (2000)
98. Gurevich A V et al. *Phys. Lett. A* **282** 180 (2001)
99. Gurevich A V, Milikh G M, Valdivia J A *Phys. Lett. A* **231** 402 (1997)
100. Gurevich A V, Milikh G M *Phys. Lett. A* **262** 457 (1999)
101. Rhodes C T et al. *J. Geophys. Res.* **99** 13059 (1994); Mazur V, Krehbiel P R, Shao X-M *J. Geophys. Res.* **100** 25731 (1995)
102. Raizer Yu P, Bazelyan É M *Iskrovoi Razryad* (Spark Discharge) (Moscow: Nauka, 1997); see also: Bazelyan E M, Raizer Yu P *Spark Discharge* (Boca Raton, Fla.: CRC Press, 1998); Bazelyan É M, Raizer Yu P *Usp. Fiz. Nauk* **170** 753 (2000) [*Phys. Usp.* **43** 701 (2000)]
103. Valdivia J A, Milikh G M, Papadopoulos K *Geophys. Res. Lett.* **24** 3169 (1997)
104. Valdivia J A, Milikh G M, Papadopoulos K *Radio Sci.* **33** 1655 (1998)
105. Iudin D I, Korovkin N B, Trakhtengerts V Yu, in *Trudy VI Vsesoyuznoi Konferentsii* (Proc. of the VI All-Russia Conf.) (Nizhnii Novgorod, 2000) p. 7
106. Russel-Dupre R et al., Report AGU Meeting, December 2000
107. Gurevich A V, Roussel-Dupre R, Zybin K P *Phys. Lett. A* **254** 79 (1999)
108. Schouland B *Proc. R. Soc. London Ser. A* **130** 37 (1930)
109. Alekseenko V V, Sborshchikov V G, Chudakov A E *Izv. Akad. Nauk SSSR Ser. Fiz.* **48** 2152 (1984)
110. Halliday E C *Proc. Camb. Philos. Soc.* **30** 206 (1934)
111. Appelton E, Bowen E *Nature* **132** 965 (1933)
112. Clay J, Jongen H, Aarts A *Physica* **28** 801 (1952)
113. Hill R J. *Geophys. Res.* **68** 6261 (1963)
114. Shaw G J. *Geophys. Res.* **72** 4623 (1967)
115. Whitmire D *Lett. Nuovo Cimento* **26** 497 (1979)
116. Angelo N D *Ann. Geophys. B* **5** 119 (1987)
117. Suszcynsky D M, Roussel-Dupre R, Shaw G J. *Geophys. Res.* **101** 23505 (1996)
118. Brunetti M et al. *Geophys. Res. Lett.* **27** 1599 (2000)
119. Abrashov S et al. *Izv. Akad. Nauk SSSR Ser. Fiz.* **50** 2203 (1986)
120. Chubenko A P et al. *Phys. Lett. A* **275** 90 (2000)
121. Gurevich A V et al. *Phys. Lett. A* **260** 269 (1999)
122. Eack K B et al. *Geophys. Res. Lett.* (2001) (in press)
123. Alexeenko V V et al., in *Proc. ICRC 2001; Copernicus Gesellschaft* 1 (2001)
124. Gurevich A V, Zybin K P *Phys. Lett. A* (2002) (in press)